The LINNEAN SOCIETY of London ZOOLOGICAL Journal of the Linnean Society

Zoological Journal of the Linnean Society, 2014, **172**, 867–891. With 11 figures

Late Palaeocene eusuchian remains from Mont de Berru, France, and the origin of the alligatoroid *Diplocynodon*

JEREMY E. MARTIN[1,2]*, THIERRY SMITH[3], FRANCE DE LAPPARENT DE BROIN[4], FRANCOIS ESCUILLIÉ[5] and MASSIMO DELFINO[6,7]

[1]*Laboratoire de Géologie de Lyon: Terre, Planètes, Environnement, UMR CNRS 5276 (CNRS, ENS, Université Lyon1), Ecole Normale Supérieure de Lyon, 69364 Lyon cedex 07, France*
[2]*School of Earth Sciences, University of Bristol, BS8 1RJ, Bristol, UK*
[3]*Direction opérationnelle Terre & histoire de la Vie, Institut royal des Sciences naturelles de Belgique, 29 rue Vautier, B-1000 Bruxelles, Belgium*
[4]*Sorbonne Universités – CR2P – MNHN, CNRS, UPMC-Paris 6, Muséum national d'Histoire naturelle, 57 rue Cuvier, CP 38, 75231 Paris cedex 05, France*
[5]*Eldonia, 9 avenue des Portes Occitanes, 03800 Gannat, France*
[6]*Dipartimento di Scienze della Terra, Università di Torino, Via Valperga Caluso 35, Torino, I-10125, Italy*
[7]*Institut Català de Paleontologia Miquel Crusafont, Universitat Autònoma de Barcelona, Edifici ICP, Campus de la UAB s/n, Cerdanyola del Vallès, Barcelona, E-08193, Spain*

Received 21 November 2013; revised 21 July 2014; accepted for publication 28 July 2014

Crocodilian remains from the late Palaeocene continental locality of Mont de Berru (Marne, France) offer the opportunity to reassess the taxonomic identity of the oldest diplocynodontid from Europe. Owing to significant morphological differences from previously described species of *Diplocynodon*, which include the presence of a splenial symphysis, a new species, ***Diplocynodon remensis* sp. nov.**, is erected here. Its inclusion in a phylogenetic framework for Eusuchia leads to its positioning as a derived member of diplocynodontids. Diplocynodontidae are viewed as a basal alligatoroid taxon, and, because morphological affinities with the Late Cretaceous–early Eocene North American genus *Borealosuchus* were mentioned in earlier studies, a comparison amongst ***D. remensis* sp. nov.**, *Leidyosuchus*, and *Borealosuchus* spp. is presented. Although ***D. remensis* sp. nov.** is the geologically oldest diplocynodontid, according to our results, it is not the phylogenetically most primitive. Other morphological discrepancies are highlighted, indicating that the topology recovered here is only tentative. From a biogeographical point of view, the appearance of *Diplocynodon* in Europe prior to the Palaeocene/Eocene boundary indicates that it did not disperse with North American taxa that reached Europe around the time of the Palaeocene-Eocene thermal maximum (PETM). Therefore, a pre-PETM dispersal from North America at the same times as other vertebrates with clear North American affinities also occurring in the Palaeocene of Europe cannot be excluded. The description of ***D. remensis* sp. nov.** adds substantial new, albeit conflicting, information, highlighting the need for a better phylogenetic framework with a revision of other critical taxa (*Menatalligator*, *Borealosuchus*) from the Palaeocene of Europe and North America.

doi: 10.1111/zoj.12195

ADDITIONAL KEYWORDS: biogeography – *Borealosuchus* – Diplocynodontidae – Europe – Eusuchia – North America.

INTRODUCTION

The fossil record of the extinct alligatoroid crocodilian *Diplocynodon* Pomel, 1847, is very abundant and limited to Europe. Recent phylogenetic results have recovered a close relationship to basal globidontans and to *Leidyosuchus canadensis* Lambe, 1907, implying a North American origin for the genus *Diplocynodon* (e.g. Brochu, 1999; Martin, 2010; Martin & Gross, 2011; Delfino & Smith, 2012) but when and how *Diplocynodon*

---

*Corresponding author. E-mail: jeremy.martin@ens-lyon.fr

dispersed to Europe is still unresolved. As recently summarized by Martin (2010) and Delfino & Smith (2012), there are eight species currently considered as valid in the age range from the early Eocene to the middle Miocene. The ancestor of *Diplocynodon* should therefore have lived earlier than the early Eocene (Martin & Buffetaut, 2008). In this respect, it is relevant that Lambe (1907) noted a morphological resemblance between *Diplocynodon* and *Leidyosuchus canadensis* Lambe, 1907, from the Late Cretaceous of North America. No Diplocynodontidae have been detected so far in the Cretaceous rocks of Europe (Martin & Delfino, 2010), or anywhere outside Europe.

The modern phylogenies (Brochu, 1999, and all those deriving from it, such as, amongst others, Brochu, 2004a, 2006a; Delfino *et al*., 2005, 2008b; Martin, 2007; Delfino, Martin & Buffetaut, 2008a; Martin & Buffetaut, 2008; Martin, 2010; Martin & Lauprasert, 2010; Martin & Gross, 2011; Brochu *et al*., 2012b) indicate that the immediate outgroup of the clade including *Diplocynodon* and Globidonta is the most basal alligatoroid *Leidyosuchus* Lambe, 1907, from North America. Close relationships between the European *Diplocynodon* (now including *Baryphracta* Frey, Laemmert & Riess, 1987; see Delfino & Smith, 2012) and the North American *Leidyosuchus* and *Borealosuchus* Brochu, 1997, have been underlined, amongst others, by Gilmore (1910) and Rauhe & Rossmann (1995). Moreover, a possible shared ancestry between the oldest – and yet undescribed – alleged *Diplocynodon*, from the late Palaeocene of Cernay-les-Reims (a locality otherwise called Berru or Mont de Berru; see Ginsburg & Bulot, 1997; Pereda-Suberbiola *et al*., 1999; Hua, 2004), and *Borealosuchus* was recently proposed by Martin (2008) and Martin *et al*. (2012).

Borealosuchus was coined by Brochu (1997) to incorporate basal eusuchians from North America previously included in the alligatoroid genus *Leidyosuchus*. There are currently six recognized species of *Borealosuchus*. *Borealosuchus sternbergii* (Gilmore, 1910) and *Borealosuchus threeensis* Brochu *et al*., 2012b, spread through the Cretaceous [but no older than late Maastrichtian, although an undescribed species was recently reported from the Campanian of Alabama (Brochu *et al*., 2012a)] to the middle Eocene. *Borealosuchus wilsoni* (Mook, 1959) is from the Wasatchian (early Eocene). The remaining species, *Borealosuchus acutidentatus* (Sternberg, 1932), *Borealosuchus formidabilis* (Erickson, 1976), and *Borealosuchus griffithi* Wu *et al*., 2001, are all Palaeocene in age (Brochu, 1997; Wu *et al*., 2001; Brochu *et al*., 2012b). The genus *Leidyosuchus* is now monospecific (Brochu, 1997), including only the Late Cretaceous *Leidyosuchus canadensis* Lambe, 1907.

The acknowledged European endemic status of *Diplocynodon* (Martin, 2010) and its hypothetical North American origins are considered in this paper. With a few Palaeocene exceptions, faunal similarities are strongest between North America and Europe during the early Eocene. This is especially remarkable for mammals, birds, and squamates (Mayr, 2009; Smith, 2009; Rage, 2012). However, a North American origin is disputed for turtles (Godinot & de Lapparent de Broin, 2003) and also crocodilians (Martin & Lauprasert, 2010), although few data are available regarding crocodilian dispersals in the Palaearctic around the Palaeocene–Eocene boundary. Following a brief review of Palaearctic Palaeocene crocodilians, we provide here a description of a new *Diplocynodon* species from the late Palaeocene [Mammal Paleogene reference level (MP6) Biochro'M, 1997] locality of Mont de Berru, analyse its phylogenetic relationships, and, it being the oldest member of the genus and the first pre-Palaeocene Eocene thermal maximum (pre-PETM) *Diplocynodon*, discuss its relevance in the context of late Palaeocene/early Eocene crocodilian biogeography.

PALAEOCENE EUSUCHIANS FROM THE PALAEARCTIC

North America certainly holds the largest published number of Palaeocene eusuchians. A few of them are known from complete gavialoid cranial material from marine deposits, with the genus *Thoracosaurus* Leidy, 1852 primarily from Cretaceous deposits (see the review in Brochu, 2004b) and the genus *Eosuchus* Dollo, 1907, from late Palaeocene deposits (Brochu, 2006b). The fossil record of freshwater ecosystems of North America is rich, and yielded mandibular remains of the basal eusuchian *Borealosuchus threeensis* from New Jersey close to the Cretaceous–Palaeocene boundary (Brochu *et al*., 2012b). More taxa have been reported from the Palaeocene, including the relatively complete skull of the alligatorine *Navajosuchus mooki* Simpson, 1930 from New Mexico, another alligatorine *Wannagosuchus brachymanus* Erickson, 1982, from North Dakota, the skull of the basal eusuchian *Borealosuchus griffithi* from Alberta (Wu *et al*., 2001), and abundant remains of *Borealosuchus formidabilis* Erickson, 1976 from North Dakota. A fragmentary taxon, *Bottosaurus* Agassiz, 1849, is also signalled from the Williamsburg Formation of the Palaeocene of South Carolina (Erickson, 1998; Brochu, 1999). Planocraniids have also been reported on the basis of fragmentary occurrences in Palaeocene deposits of North America (Brochu, 2013). In comparison, the Palaeocene Asiatic fossil record is more fragmentary (see Martin & Lauprasert, 2010), with poorly known taxa known only from freshwater settings of China, such as the crocodyloid *Asiatosuchus nanlingensis* Young, 1964. *Eoalligator chunyi* Young, 1964, is considered to be a junior synonym of *Asiatosuchus nanlingensis* Young, 1964 (C. A. Brochu, pers. comm. 2014) and *Eoalligator huiningensis* Young, 1982, clearly needs a reappraisal. Other Palaeocene eusuchians from Asia are represented by two species of the genus *Planocrania* (see details in Brochu, 2013).

Fewer Palaeocene localities containing eusuchians have been found in Europe does not stand as a better supply for Palaeocene localities and it can be qualified as scarce, especially during the earliest Palaeocene, when it mainly consists of gavialoid taxa found in nearshore environments such as *Thoracosaurus* sp. from Poland (Zarski, Jakubowski & Gawor-Biedowa, 1998) and *Thoracosaurus isorhynchus* (Pomel, 1847) from Mont-Aimé, Champagne-Ardenne, France. In the late Palaeocene, the marine record is represented by the gavialoid *Eosuchus lerichei* Dollo, 1907 (Delfino *et al*., 2005) from northern France. Such a bias in the nonmarine eusuchian fossil record is linked to the fact that early Palaeocene continental deposits from Europe are rare (Godfriaux & Thaler, 1972; Thaler, 1977; Peláez-Campomanes *et al*., 2000; Domingo *et al*., 2007; De Bast & Smith, 2013) and have only yielded a few eusuchian remains from the early Palaeocene locality of Hainin in Belgium (Groessens-Van Dyck, 1986). The second oldest occurrence of a freshwater crocodilian in the European Cenozoic may be from the late Palaeocene of Menat, Massif Central, France, where a single specimen lacking most of the skull but preserving a nearly complete postcranium was given the name *Menatalligator bergouniouxi* Piton, 1940. The description mentions a dorsal and a ventral shield with imbricated elements, features compatible in Europe with *Diplocynodon*. However, the specimen is now considered lost. A last European Palaeocene locality has been mentioned several times in the literature for its crocodilian fauna: Mont de Berru (also known as Cernay-les-Reims), a freshwater deposit of the upper Thanetian (MP6) of the Paris Basin, located in north-eastern France. An *Asiatosuchus*-like crocodyloid (Vasse, 1992, 1993; Delfino & Smith, 2009), together with mandibular remains regarded as the earliest occurrence of the alligatoroid genus *Diplocynodon* (Ginsburg & Bulot, 1997; Pereda-Suberbiola *et al*., 1999; Hua, 2004), were reported from this locality. Here we report on several specimens from this locality, including complete skulls and mandibles referable on a morphological basis to the same taxon previously mentioned on the basis of mandibular fragments (Hua, 2004). In Europe, the diplocynodontid lineage extends back beyond the mid-Eocene, being reported from the early Eocene of France, Portugal, and Belgium (Godinot *et al*., 1978; Telles-Antunes & Russell, 1981; Buffetaut, 1985; Hua, 2004; Smith *et al*., 2014); the knowledge of the precise relationship of the diplocynodontid lineage with the earliest crocodilian faunas suffers from a gap covering most of the Palaeocene. The present study was aimed at reducing these phyletic and temporal gaps.

INSTITUTIONAL ABBREVIATIONS

CE, Collection Eldonia, Gannat, France; IRSNB, Institut royal des Sciences naturelles de Belgique; MGPT, Museo di Geologia e Paleontologia of the University of Torino; MHNL, Musée des Confluences de Lyon, Lyon, France; MNHN F BR, Muséum National d'Histoire Naturelle – Berru collection, Mourras quarry of Mont de Berru, Paris, France; MNHN F CRL, Muséum National d'Histoire Naturelle – Conglomérat de Cernay of Lemoine collection and quarry of Mont de Berru, Paris, France.

SYSTEMATIC PALAEONTOLOGY

ORDER CROCODILIA GMELIN, 1789 *SENSU* MARTIN & BENTON, 2008

SUBORDER EUSUCHIA HUXLEY, 1875

SUPERFAMILY ALLIGATOROIDEA GRAY, 1844

FAMILY DIPLOCYNODONTIDAE HUA, 2004

GENUS *DIPLOCYNODON* POMEL, 1847

Emended diagnosis: The following character combination is diagnostic of the genus *Diplocynodon* (plesiomorphies indicated with an asterisk): a pair of enlarged maxillary (four and five) and confluent dentary (three and four) alveoli*; lacrimal longer than prefrontal*; ectopterygoid adjacent to the posteriormost maxillary alveoli*; dorsal margin of the infratemporal fenestra formed by the quadratojugal, preventing the quadrate from reaching the fenestra; 16–17 maxillary alveoli. Autapomorphies recovered from phylogenetic analyses diagnose *Diplocynodon* by: axial hypapophysis located toward the centrum; proatlas with tall dorsal keel; dorsal margin of the iliac blade rounded in shape, with a smooth border and a very deep posterior tip of the blade; lingual foramen for the articular artery and alveolar nerve perforates surangular/angular suture; quadrate–pterygoid suture linear from basisphenoid exposure to foramen ovale.

***DIPLOCYNODON REMENSIS* SP. NOV.**

Etymology

The species name refers to the Gallic natives: the Remes who inhabited the region of Reims from where the fossil was recovered.

Holotype

MHNH F BR 4020, a nearly complete skull (Fig. 1C, D).

Type locality

Mont de Berru, Mourras quarry, between Cernay-les-Reims and Berru villages, Département de la Marne, Champagne-Ardenne, north-eastern France (see map in Russell, 1964).

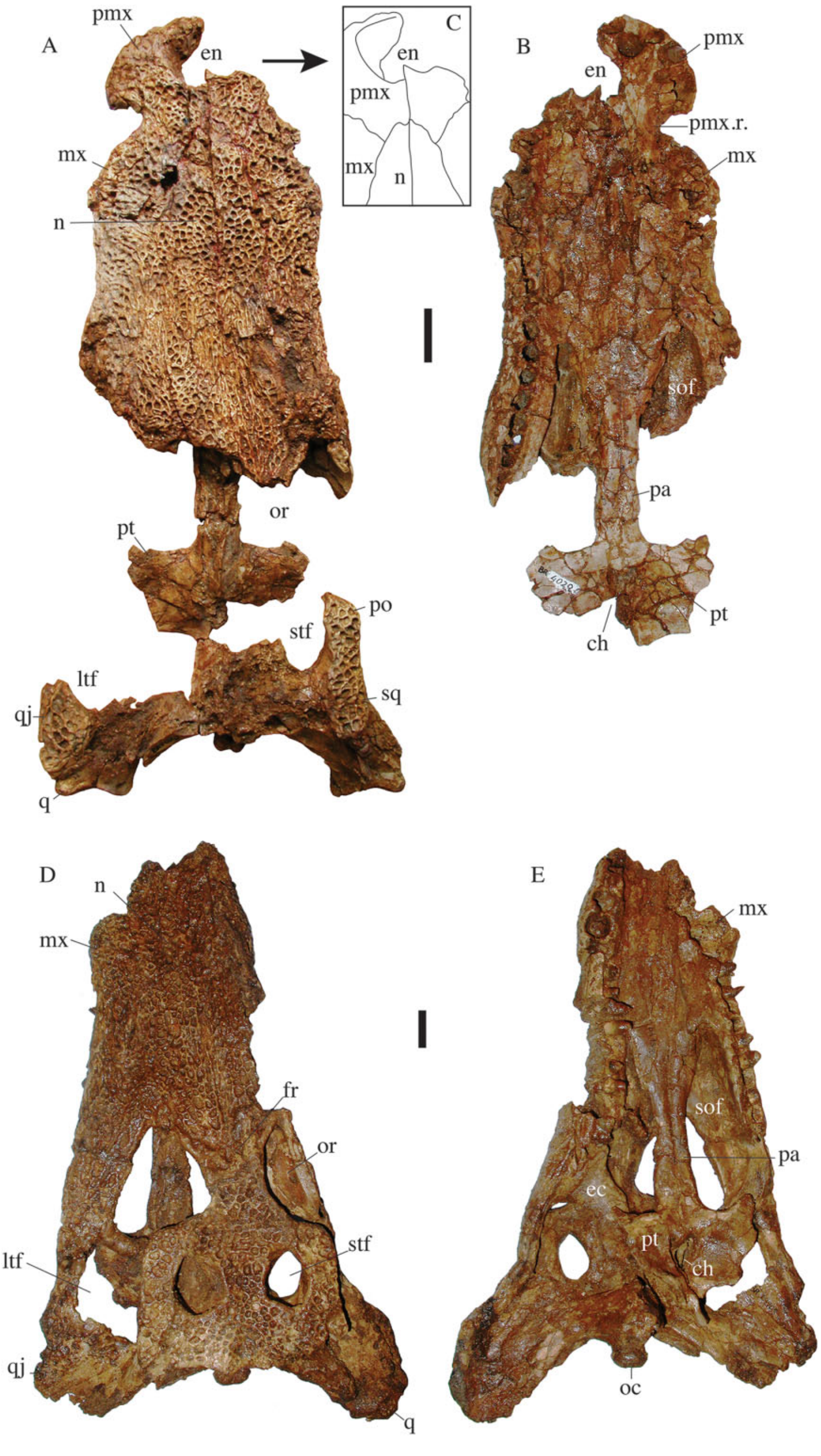

Figure 1. Skulls of ***Diplocynodon remensis* sp. nov.** from the Late Palaeocene of Mont de Berru. MHNH F BR 4020 (holotype) in A, dorsal and B, ventral views. Most sutures were imperfectly observed and are therefore not indicated with the exception of the anterior portion of the rostrum of the holotype MNHN BR 4020 showing in C, the exclusion of the nasals from the posterior margin of the external nares by the medially connecting premaxillae, as seen in other species of *Diplocynodon*; MNHN F BR 13105 in D, dorsal and E, ventral views. Abbreviations: ch, choanae; ec, ectopterygoid; en, external nares; fr, frontal; ltf, lower temporal fenestra; mx, maxilla; n, nasal; oc, occipital condyle; or, orbit; pa, palatine; pmx, premaxilla; pmx.r., premaxillary recess; po, postorbital; pt, pterygoid; q, quadrate; qj, quadratojugal; sof, suborbital fenestra; sq, squamosal; stf, supratemporal fenestra. Scale bars = 2 cm.

Type horizon

A fossiliferous level intercalated in sands, between Sables de Rilly and lacustrine blue-grey marls (Russell, 1964), approximate continental equivalent of the Châlons-sur-Vesles marine Formation (see Aubry *et al*., 2005), Paris Basin. Upper Thanetian, Late Palaeocene, MP6 reference-level of the mammalian biochronological scale for the European Palaeogene (Biochro'M, 1997).

Referred specimens

From the type locality Mourras quarry and Lemoine quarry (same level), Mont de Berru, Départment de la Marne, Champagne-Ardenne, north-eastern France: skull (incomplete): MNHN F BR 4020, 13105 (Fig. 2A–D); skull and associated mandibles (complete): CE 00001 (Figs 2–5); skull fragment (posterior region): MNHN F BR 13106; premaxilla.

MNHN F BR 3501, 13202, 15012, 15142; maxilla.

MNHN F BR 1960, 2632, 2634, 2636, 2637, 3486, 13207, 13228, 13229, 13231, 13679, 13711, 15013, 54435, MNHN F CRL 13099, IRSNB Vert 29857-7; nasals: MNHN F BR 3488, 13200, 13201, 15079; prefrontal.

MNHN F BR 3490; lacrimal.

MNHN F BR 1694; postorbital.

MNHN F BR 2628, 3505, 3526; squamosal.

MNHN F BR 2619, 2621, 3425, 13210, 13211, 15260; jugal.

MNHN F BR 2620, 3500, 3507, 3511, 3527, 3595, 13212, 13213, 13214, 13215, 15049, 15477, IRSNB Vert 29857-8 to 9; frontal.

MNHN F BR 2616, 3297, 3489, 3496, 3497, 13208, 13209, 13676, 13677, 13681, IRSNB Vert 29857-10 to12; frontal + parietal + prefrontal + supraoccipital.

MNHN F BR 3591; exoccipital + quadrate.

MNHN BR 3513, 4139; exoccipital + frontal + laterosphenoid (?) + parietal + quadrate + supraoccipital.

MNHN BR 2622; quadrate.

MNHN F BR 3493, 3504, 3510, 13189, 13190, 13191, 13192; basioccipital.

MNHN F BR 4119; palatine.

MNHN F BR 13205; pterygoid.

MNHN F BR 15200, 15476; ectopterygoid.

MNHN F BR 1645; dentary.

MNHN F BR 1974, 2617, 2618, 2629, 3503, 3506, 3523, 4021, 4037, 13056, 13216, 13217, 13218, 13219, 13220, 13221, 13222, 13223, 13224, 13225, 13226, 13227, 13237, 15198, 15230, 15231, 15232, 15471, 15472, MNHN F CRL 13097, 13098, IRSNB Vert 29857-13 to 15; splenial.

MNHN F BR 4153, 10271, 13203, 15150; angular.

MNHN F BR 1673, 1963, 1973, 2635, 3499, 3508, 3608, 13193, 13194, 13195, 13196, 13198 (= 3502), 13199, 15166, 15187, 15247, 15473, 15474, IRSNB Vert 29857-16 to 18; surangular.

MNHN F BR 1675, 2623, 3487, 13206, MNHN F BR no number; articular.

MNHN F BR 3596, 10146, 10527, 12456, 12485, MNHN F BR no number, MNHN F CRL 13051; several isolated teeth (unnumbered MNHN); osteoderm: MNHN F BR 2654, 2653, 3432, 3456, 3465, 3467, 3470, 3471, 13712, 15084, 15176, 15478, 15480, 15481, 17412, 17413 and about 300 unnumbered osteoderms), IRSNB Vert 29857-19 to 40; IRSNB R289 (IG 26857), two partial dentaries in connection (Fig. 7A, B); MGPT-PU 132047, STereoLithography (STL) file of the computed tomography (CT) scan of the skull and mandible of CE 0001.

Diagnosis

Diplocynodon remensis differs from all other species of *Diplocynodon* by possessing two parallel ridges creating a recess on the lateral wall of the premaxillary notch; and in having a splenial participating in the mandibular symphysis.

Description

General description

Diplocynodon remensis is a medium-sized crocodilian (see Table 1 for skull measurements) that may not have exceeded 2 m in total length. The skull shows the platyrostral condition, with a narrow snout. Nearly all skull remains have suffered from dorsoventral crushing. Although many small fractures run across the bones of all specimens, the quality of preservation offers nicely preserved morphological details. A 'net' of pits with well-delimited narrow ridges rather uniformly covers the dorsal surface of the skull. Pit size is variable, the skull table displaying the largest ones whereas pits near the margin of the jaws tend to become smaller or absent. In dorsal view, the shape of the skulls is elongated and the premaxillary–maxillary region is characterized by a pronounced lateral embayment at the level of the suture between these two elements. On the external surface, canthii rostralii or preorbital ridges are not developed but a marked spectacle is present in the interorbital area: it consists of a transverse step crossing the frontal at or just anteriorly to the posterior end of the fronto–prefrontal suture and by two symmetrical depressions running along the anteromedial edges of the orbits, medially delimited by a thin, continuous ridge (such depressions are like elongated pits of the skull ornamentation; MNHN F BR 3591 and CE 00001 clearly preserve a complete 'spectacle'). A tubercle-like structure is present on the lacrimal at the anterior tip of the orbit.

Skull

Premaxilla: The premaxilla is about 1.5 times longer than wide. Dorsally, the anterior portion is smooth, whereas pits densely cover the posteromedial portion. The premaxilla completely surrounds the external nares. The dorsally facing nares are large, roughly rounded,

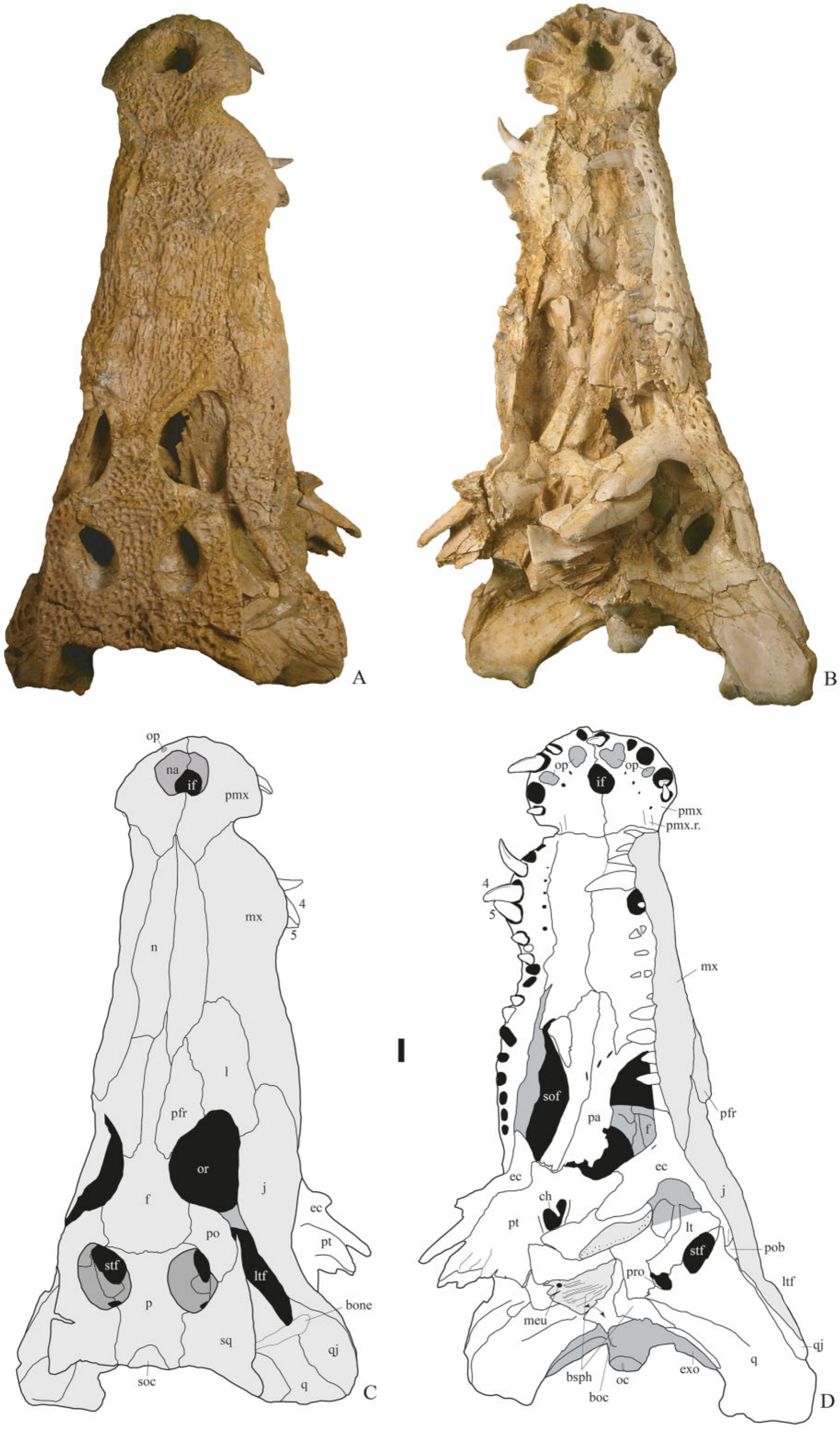

Figure 2. Photographs and line drawings of the skull of ***Diplocynodon remensis* sp. nov.** (CE0001) from the Late Palaeocene of Mont de Berru in dorsal (A, C) and ventral views (B, D). Abbreviations: 4, 5, tooth or alveolus position in the maxilla or dentary; boc, basioccipital; bsph, basisphenoid; ch, choanae; ec, ectopterygoid; exo, exoccipital; f, frontal; if, incisive foramen; j, jugal; l, lacrimal; lt, laterosphenoid; ltf, lower temporal fenestra; meu, median Eustachian canal; mx, maxilla; n, nasal; na, naris; oc, occipital condyle; op, occlusal pit; or, orbit; p, parietal; pa, palatine; pfr, prefrontal; pmx, premaxilla; pmx.r., premaxillary recess; po, postorbital; pob, postorbital bar; pro, prootic; pt, pterygoid; q, quadrate; qj, quadratojugal; soc, supraoccipital; sof, suborbital fenestra; sq, squamosal; stf, supratemporal fenestra. Scale bar = 1 cm.

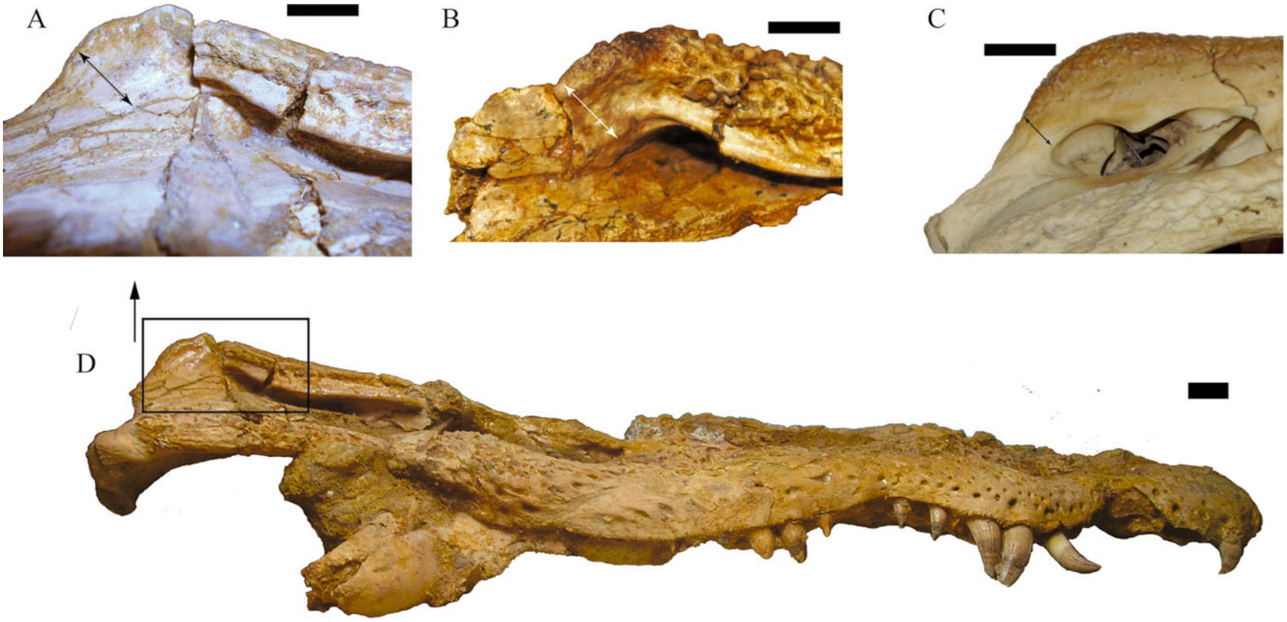

Figure 3. Comparison of the otic area in ***Diplocynodon remensis*** **sp. nov.** and other crocodilians: A, detail of the right otic area of CE 0001 and comparison with the same area from B, MNHN F BR 4020 and C, an adult skull of *Crocodylus niloticus* (MHNL 50.001388); D, right lateral view of ***D. remensis*** **sp. nov.** (CE 0001) from the Late Palaeocene of Mont de Berru. The small double arrows allow comparison of the relative width of the squamosal behind the otic aperture. Scale bars = 1 cm.

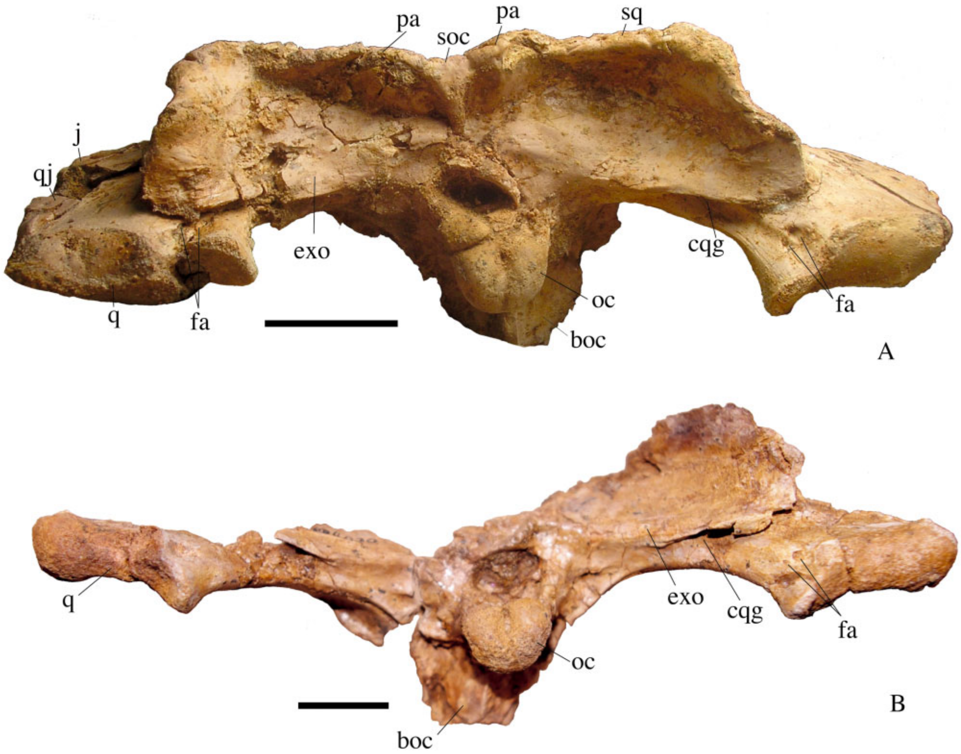

Figure 4. The skull of ***Diplocynodon remensis*** **sp. nov.** in occipital view from specimens A, CE 0001 and B, the holotype MNHN F BR 4020. Abbreviations: boc, basioccipital; cqg, cranioquadrate groove; exo, exoccipital; fa, foramen aëreum; j, jugal; oc, occipital condyle; pa, palatine; q, quadrate; qj, quadratojugal; soc, supraoccipital; sq, squamosal. Scale bars = 2 cm.

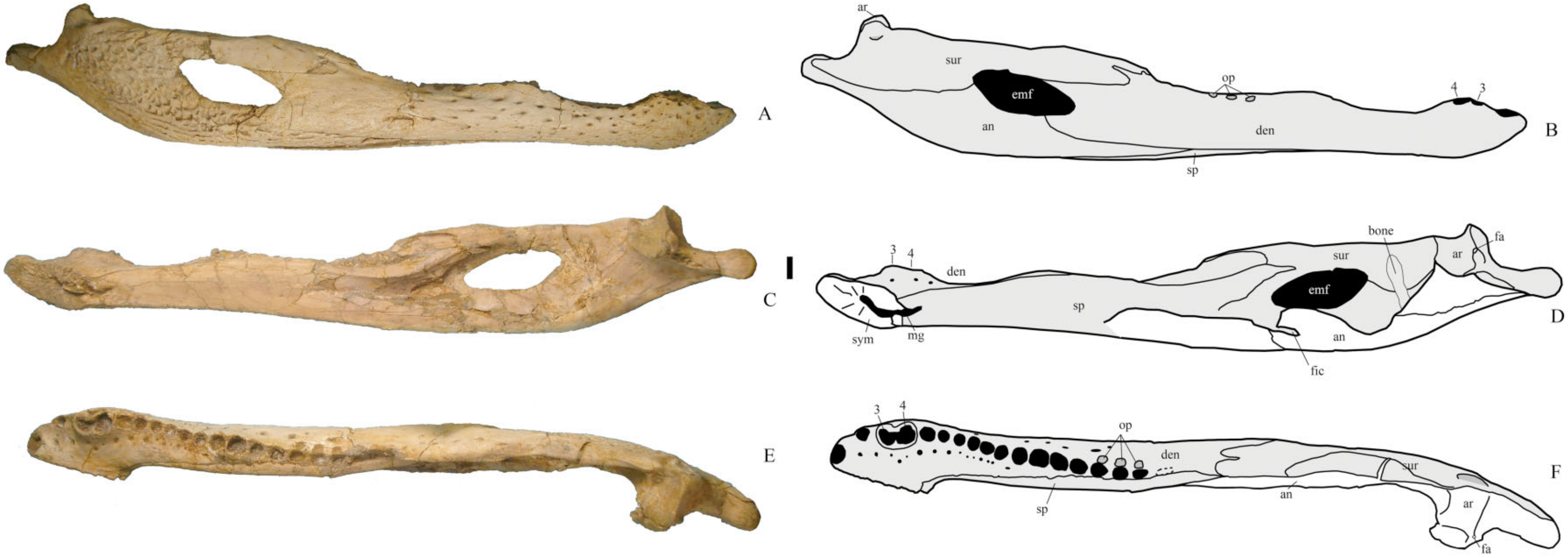

Figure 5. Photographs and line drawings of the right mandible of ***Diplocynodon remensis* sp. nov.** (CE) from the Late Palaeocene of Mont de Berru in lateral (A, B), medial (C, D), and dorsal views (E, F). Abbreviations: 3, 4, tooth or alveolus position in the maxilla or dentary; an, angular; ar, articular; den, dentary; emf, external mandibular fenestra; fic, foramen intermandibularis caudalis; mg, Meckelian groove; op, occlusal pit; sp, splenial; sur, surangular; sym, symphysis. Scale bar = 1 cm.

Table 1. Skull measurements of *Diplocynodon remensis* (complete skull CE0001)

Feature	Measurement (mm)
Premaxilla to posterior skull table length	298
Interorbital width	22
Anteroposterior supratemporal length	33
Mediolateral supratemporal length	22
Cranial table width	90
External interquadrate width	162
Maxillary width at level of confluent teeth	80
Orbital length	48
Orbital width (right)	33

and positioned closer to the anterior margin of the premaxilla than of the premaxillary–maxillary notch. The posterior premaxillary process extends behind the level of the premaxillary–maxillary notch to the level of the second maxillary tooth. The snout profile can be described as deeply notched, contrary to what is observed in diplocynodontids or in globidontans. Here, posteriorly in the notch, the lateral margin of the premaxilla becomes perpendicular to the sagittal plane. On the ventral side, the incisive foramen is slightly longer than wide. It is excluded from the tooth row. As also shown by the isolated premaxillae, as well as by the right maxilla MNHN F BR 15013, the premaxilla–maxillary suture is approximately rectilinear on the palatal surface (only modestly convex anteriorly), therefore remaining far from the incisive foramen and not extending posteriorly to the first maxillary alveolus. The premaxilla bears five alveoli. The first, second, and fifth alveoli are the smallest of all and are the same size. The third and fourth are three times larger. A large occlusal pit is located between the first and second alveoli. A second occlusal pit is three times smaller and positioned between the third and fourth alveoli. Small foramina are usually present medially to the alveoli. Behind the last premaxillary alveolus, the premaxilla is deeply notched for reception of the double caniniform dentition of the dentary. Here, the smooth surface of the premaxilla bears two parallel longitudinal ridges (Figs 3, 6H, I, J) that are well marked in the large MNHN F BR 4020 and MNHN F BR 3501 but barely visible in the smaller MNHN F BR 15012. Such notch is mostly developed on the premaxilla and only the posterior sector of the notch involves the maxilla.

Maxilla: The maxilla is craniocaudally elongate. Dorsally, it is densely covered with pits. In dorsal view, the lateral profile of the maxilla in CE 00001 and MNHN F BR4020 is progressively extending laterally from the notch until the level of the fourth and fifth double caniniform maxillary teeth. A concave wave affects the tooth row to the level of the eighth maxillary tooth and then the lateral edge of the maxilla becomes straight for the rest of the bone. The suture with the nasal is almost straight. The posteromedial maxillary suture extensively contacts the lacrimal. In the maxillae of CE 00001, 18 alveoli are visible and this is confirmed by the CT scan. The tooth row preserves 17 alveoli in the right maxilla of the skull MNHN F BR 4020 (the left one is not entirely preserved) and in the isolated left maxilla MNHN F BR 13207 (Fig. 6F), but the same count is also likely to be correct for MNHN F BR 2636 (Fig. 6E) and MNHN F BR 2637 whose distal regions are slightly damaged and miss the last two alveoli. The tooth row nearly reaches the posterior end of the maxilla. The first maxillary alveolus is as small as the fifth premaxillary tooth. The second and third alveoli are larger in diameter. Next, the fourth and fifth alveoli, corresponding to the double caniniform teeth, are even larger and of same size and nearly confluent. Posteriorly, the remaining alveoli are of similar diameter, although a slight increase in diameter affects the 12th alveolus together with an obvious festoonation of the posterior maxillary tooth row. The last four alveoli are slightly mediolaterally compressed. The largest interalveolar space is usually the seventh and it corresponds to a large pit. The foramen for the palatine ramus of the fifth cranial nerve is present and smaller than the alveoli but not tiny (best seen in MNHN F BR 2636 where it is about 5 mm long); several other small foramina are aligned medially to the tooth row. Along the suborbital fenestra, the area medial to the tooth row (and anterior to the overlap surface with the ectopterygoid) is modestly but clearly expanded in a medial direction, giving a slightly convex shape to the lateral rim of the fenestra (Figs 1, 6E–G): this character is slightly variable, being nearly not present in MNHN F BR 13207 (however, the weak expansion is not visible in dorsal view because of the deformation of the specimen) but evident in MNHN F BR 2636, MNHN F BR 2637, MNHN F BR 4020, MNHN F BR 13105, and MNHN F BR 13679. Unlike in some other alligatoroids, there is no maxillary shelf separating the posterior maxillary tooth row from the ectopterygoid and although the condition is not exactly comparable with that of *Crocodylus*, it is clear that, as in other species of *Diplocynodon*, the last two maxillary alveoli are in contact with the ectopterygoid (e.g. Martin, 2010). The state of preservation does not allow the presence or absence of pits in the narial canal to be assessed with confidence; however, MNHN F BR 3486 preserves a portion of the canal without pits disrupting the medial wall of the maxillary cavichoncal recess.

Nasal: The nasals are very elongate, covering most of the snout length. They do not enter the naris, being widely separated from it (in CE 00001 more than 2 cm

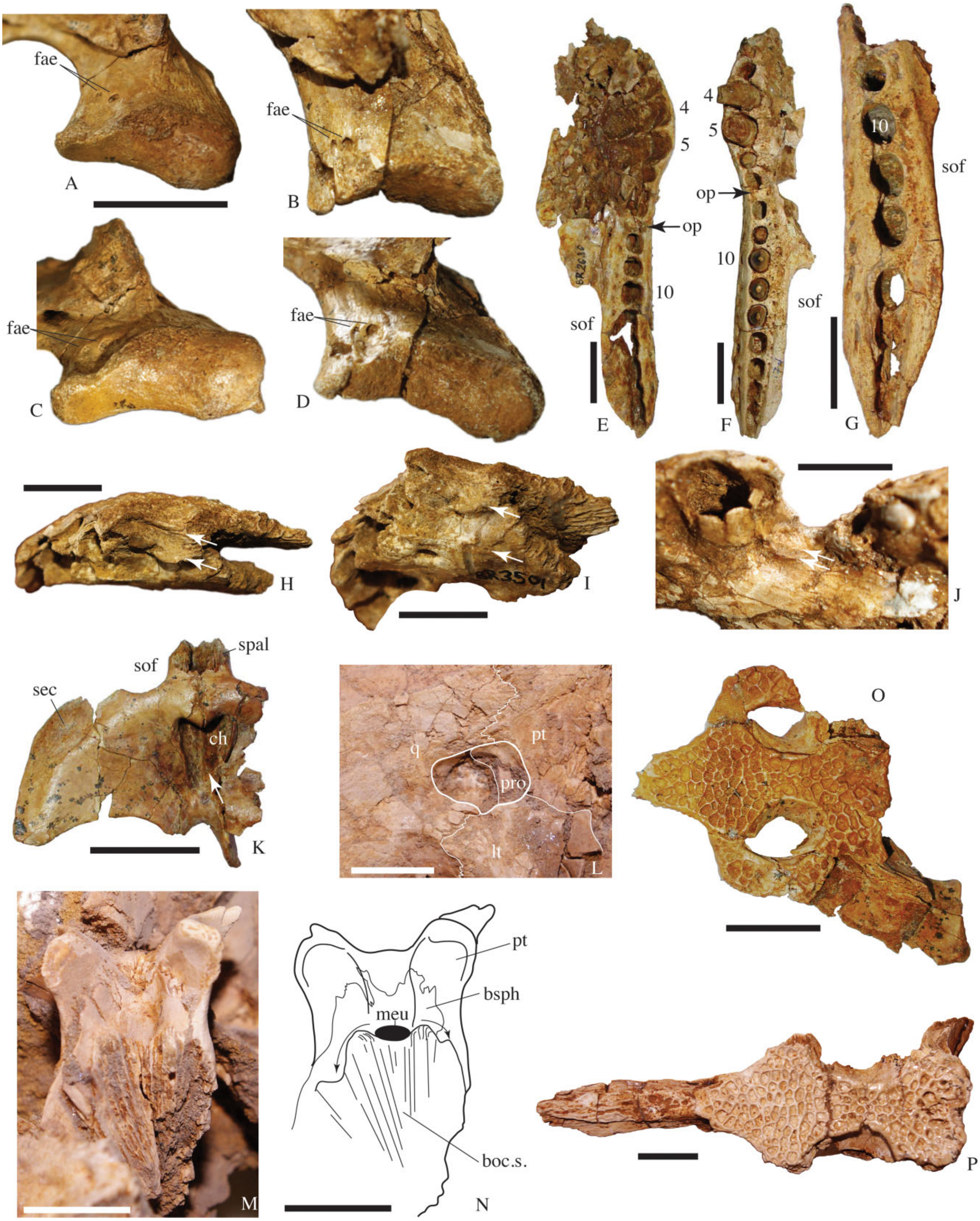
fae
A
fae
B
fae
C
fae
D
4
5
op
10
sof
E
4
5
op
10
sof
F
10
sof
G
H
I
J
sof
spal
sec
ch
K
q
pt
pro
lt
L
O
M
pt
bsph
meu
boc.s.
N
P

Figure 6. Selected skull details of ***Diplocynodon remensis* sp. nov.** A–D, quadrates in dorsal (A, B) and posterodorsal (C, D) views of MNHN F BR 3513 (A, C) and MNHN F BR 4020 (B, D); note the double perforation. E–G, maxillary tooth rows of MNHN F BR 2636 (E), MNHN F BR 13207 (F), MNHN F BR 13679 (G). H–J, details of left premaxillary–maxillary notches in lateral and ventral views of MNHN F BR 3501 (H and I with slightly different views) and MHNH BR 4020 (J); the double arrows point to the double longitudinal recess. K, pterygoid plate in ventral view of MNHN F BR 13100, the arrow indicates the septum; L, details of the left prootic area in CE 0001; M, the basisphenoid of CE 0001 in posterior view and N, associated reconstructed sutures; the two arrows follow the gutter leading to the lateral Eustachian openings. O, skull table of MNHN F BR 13106. P, partial skull table and frontal of MNHN BR 2622 showing the frontoparietal suture. Abbreviations: 4, 5, 10, tooth or alveolus position in the maxilla or dentary; boc.s., basioccipital suture of the basisphenoid; bsph, basisphenoid; ch, choanae; fae, foramen aëreum; lt, laterosphenoid; meu, median Eustachian canal; op, occlusal pit; pro, prootic; pt, pterygoid; q, quadrate; sec, suture for ectopterygoid; soc, supraoccipital; sof, suborbital fenestra; spal, suture for palatine. All scale bars = 2 cm except 1 cm in L, M, and N.

◄

of premaxillary surface). They are densely covered with rounded pits but the dorsal ornamentation slightly varies between the proximal and the distal end: the proximal sector shows elongated ridges delimiting furrows conjoining the pits, whereas pits are isolated in the median and distal sectors. The nasals have a somehow constant width and they become abruptly narrow toward their anterior end. The nasals are medially separated in their posterior region by a slender anterior frontal process. The posterior nasal process reaches the medial side of the lacrimal and of the right prefrontal (Fig. 2) with an oblique and short suture.

Lacrimal: The lacrimal participates in the anteriormost portion of the orbital rim. The bone is longer than wide. The anterior limit of the lacrimal reaches a more anterior position than that of the prefrontal and therefore it extensively contacts the posterior end of the nasal. The preorbital ridge terminates on the posteromedial corner of the lacrimal. The right lacrimal MNHN F BR 1694 has a smooth, triangular surface and preserves the anterolateral orbital margin. A small but evident knob is present at the anterior tip of the smooth, triangular surface (such a structure is also present on the lacrimals of the two skulls MNHN F BR 4020, 13105). The lacrimal duct is located medially to the anterior rim of the orbit, close to the suture with the prefrontal, and opens anteriorly on the ventral surface of the element, with a large aperture.

Prefrontal: The prefrontal is very elongate, shorter and narrower than the lacrimal, and forms the anteromedial portion of the orbital rim. Its anterior tip does not surpass the anterior tip of the frontal process (see MNHN F BR 3591). Its anterior portion inserts between the nasal and lacrimal. The orbital margin is inflated at the level of this bone and consists of the lateral branch of the preorbital ridge. The suture with the lacrimal is almost straight. Prefrontal pillars are not preserved except in the skull MNHN F BR 4020 where the left pillar is visible in dorsal view, and the right one seems to be anteroposteriorly expanded at its dorsal end; the medial process is broken off.

Jugal: The jugal makes up the lateral margin of the orbital rim as well as the lateral margin of the infratemporal fenestra. The orbital portion of the jugal is wide whereas it becomes thin in the distal region. In ventral view, the posterior extension of the ectopterygoid extends along the jugal. Extension of the jugal on the postorbital bar is obscured by crushing. In all of the jugals, the postorbital bar is inset from the lateral jugal surface, but in the area anterior to the postorbital bar, the lateral wall is weakly developed dorsally (in particular, not as developed as in *Diplocynodon ratelii*). The medial jugal foramen is always present: when only one foramen is present, its size is large (MNHN F BR 13215, 15477, 2620, 3595, 13214; both the jugals of skull MNHN F BR 13105) but when more foramina are present, their size varies from medium (MNHN F BR 3511, 3527, 13213) to small (as in the case of the three foramina of the large jugal MNHN F BR 13212). Some jugals (MNHN F BR 3500, 3507, 15049) have a damaged foraminal area: it is possible that the presence of a large foramen renders the area rather fragile. The posterior extension of the jugal on the quadratojugal does not reach the level of the quadrate condyle. The quadratojugal suture is not obvious but seems to attain the caudal angle of the infratemporal fenestra. MNHN F BR 15049 and MNHN F BR 2620 have a sutural area for a rather long process of the quadratojugal that extends along the lower temporal bar along the medial surface of their posterior end (not completely preserved).

Frontal: In CE 00001, the frontal contacts the parietal in front of but close to the supratemporal fenestrae, although the left frontal seems to intersect the fenestrae. In BR13105, the frontoparietal suture enters the anterior margin of the supratemporal fenestra. The frontoparietal suture is slightly undulating. The postorbital and parietal retain a small contact on the anterior margin of the supratemporal fenestra. The dorsal surface of the frontal is completely flat on the skull table and between the orbits; it is not elevated either along the rims of the orbits or along the supratemporal fenestrae. The parietal forms the anteromedial margin of the supratemporal fossae as the frontoparietal suture is not entirely developed on the skull table but instead enters the fossae below. The interorbital region is wide. At this level, the frontal becomes constricted between the prefrontals and sends a long and slender anterior process, which projects far beyond the anterior orbital level, as well as beyond the anterior level of the prefrontal. The anterior frontal process eventually divides the paired nasals in their posterior region.

Postorbital: The postorbital makes up the anterolateral border of the supratemporal fenestra. The anterior region does not extend very much medially and the bone is more elongate than wide. The supratemporal border is vertical. The dorsal surface of the bone is flat. The postorbital bar is thick but is not as massive as in *Gavialis*. It is laterally directed with respect to the dorsal surface of the element, such that it can be seen in dorsal view (MNHN F BR 2628).

Parietal: The parietal is entirely flat dorsally and is constricted between the supratemporal fenestrae. The space between the supratemporal fossae is barely narrower than the interorbital space. The parietal contribution to the posterior border of the skull table is limited by the supraoccipital, which is exposed on the skull roof dorsal surface. The suture with the squamosal does not extend far laterally and gives a continuous parasagittal orientation to the outline of the parietal. The lateral margin overhangs the fenestra with various degrees of development, as observed in the different specimens available. No ridge delimits the supratemporal border. The posterior surface of the supratemporal fenestra is perforated by the orbitotemporal foramen. The organization around this foramen can be seen from the left temporal cavity of CE 00001 and in BR13105. Here, the parietal and squamosal are in contact, preventing the ascending quadrate process from reaching the ventral margin of the foramen.

Squamosal: The squamosal makes up the posterolateral corner of the supratemporal fenestra. As for any other bone from the skull table, the squamosal dorsal surface is flat. The squamosal is wide, occupying most of the posterior surface of the skull table. Squamosal prongs are developed but they do not reach the lateral tip of the paroccipital processes (best preserved in MNHN F BR 4020) and thus do not project far posteriorly. The caudal margin of the otic aperture is long and continuous with the paroccipital process, unlike the condition seen in derived eusuchians, in which the otic aperture is deeply inset from the paroccipital process (Fig. 3). In the isolated elements MNHN F BR 2619 and MNHN F BR 15260, the sutural area with the quadrate considerably extends in an anterodorsal direction, indicating that the squamosal constitutes only the uppermost dorsal section of the posterior rim of the otic recess. On the lateral sides of squamosals, the rims of the groove for the musculature connected to the external otic aperture are approximately parallel; the dorsal rim is extremely ornate (as is the dorsal surface); the ventral rim typically has a lateral expansion (approximately in the middle).

Palatine: The paired palatines comprise the median walls of the suborbital fenestrae and project rostrally within the maxillae to the level of the eighth and ninth alveoli. Caudally, until half of their length, the palatines have parallel margins. At this level, there is no lateral flaring of the bone. They eventually become wider from their second halves and start to expand laterally to contribute about one third to the length of the anterior suborbital margin. The palatine projection within the maxillae is rather long and wide. The palatine–pterygoid suture is located well ahead of the posterior corner of the suborbital fenestra as clearly seen in CE 00001, MNHN F BR 4020, MNHN F BR 13105, and MNHN F BR 15200.

Ectopterygoid: The ectopterygoid contacts the posteriormost portion of the maxillary tooth row by its dorsal anterior process, which is short. Its real anterior extension is unclear but it may have reached at least the last two alveoli. There is no outgrowth of the maxilla preventing the ectopterygoid from touching the posterior tooth row. The dorsal posterior process of the ectopterygoid is twice as long as the anterior process; it runs along the medial jugal margin and therefore participates in at least the anteroventral infratemporal margin. The ventral ectopterygoid process is massive and does not project all the way to the tip of the pterygoid wing. Instead, it stops at more than half the distance. The contact with the pterygoid is difficult to assess because of deformation. This suture is curved, with the ectopterygoid being overlapped by the pterygoid. The pterygoid ramus of the ectopterygoid is bowed medially so that the posterolateral margin of the suborbital fenestra is concave.

Pterygoid: The pterygoid edge contributing to the posterior rim of the suborbital fenestra does not show any notch. The choanae open in the central region of the pterygoids, forming a rounded canal, the margins of which are slightly deformed. Its lateral margins form a collar, the pterygoid being depressed lateral to it (particularly visible in MNHN F BR 15200). From the anterior border of the choanae, a well-developed septum invaginates into the canal. The pterygoid posteromedial process forms a distinct and developed notch. The posteromedial pterygoid process extends more caudally than the pterygoid wings. The pterygoid wings are massive with a thick margin for reception of the ectopterygoid. These wings are wider than long.

Quadrate: The quadrate does not participate in the infratemporal fenestra. Its exposed surface is smooth.

It does not project far posteriorly beyond the skull table level. From an occipital point of view, the medial quadrate hemicondyle is very diminutive compared with the lateral one. On the dorsal surface of the bone, the foramen aëreum is medially placed (Fig. 6A–D). In ventral view, the quadrate is well exposed. Its surface is smooth and is only elevated by a faint muscle scar (scar B of Iordansky, 1973). Anteriorly, the quadrate penetrates the ventral margin of the supratemporal fenestra.

Quadratojugal: The quadratojugal makes up the dorsal margin of the infratemporal fenestra where it is free of sculptural pits. It laterally contacts the posterior-most extension of the quadrate and displays well-developed pits. Dorsally, the rostral-most process of the quadratojugal contacts the postorbital bar, thus excluding the quadrate from the lower temporal fenestra. No spina quadratojugalis was detected in any quadratojugal, but its presence cannot be completely rejected.

Supraoccipital: The unpaired supraoccipital is massive and extends within the parietal on the dorsal surface of the skull table. It however does not exclude the lateral margins of the parietal from contacting the posterior margin of the skull table. In most cases, the supraoccipital corresponds to a weak depression on the skull table and from an occipital view, the dorsal surface of the supraoccipital is concave. Its lateral-most extension plunges below the skull table surface and has a process that extends into the squamosal. The dorsal surface of this element is well developed in the posterior direction (it extends posteriorly to the concave posterior rims of the parietals) and markedly overhangs the occipital skull surface contributing, with the parietals, to the overall convex shape of the median sector of the posterior edge of the skull table. A strong-keeled descending process penetrates between the paired exoccipitals but does not prevent them from meeting completely. The supraoccipital medially delimits the post-temporal fenestrae but information on their detailed morphology is not available in any of the remains.

Exoccipital: The exoccipital makes an extensive participation to the occipital region. The otoccipital process is long and in its central and lateral part overhangs the cranioquadrate canal. This canal is enclosed laterally by the quadrate and bound medially by the exoccipital. The exoccipital extends more laterally than the squamosal. The descending process of the exoccipital does not project along the lateral side of the basioccipital plate, but instead is short and stops near the level of the condyle. The exoccipitals form the dorsal and lateral rim of the foramen magnum and extend laterally below the squamosal prongs forming the paroccipital processes. The occipital surface of these processes is rather concave and its ventral edge is somewhat straight. No boss is developed on the paroccipital processes but a weak ridge is present medially to the opening of the cranioquadrate passage. The group of foramina positioned on the ventral projections of the exoccipitals, laterally and lateroventrally to the foramen magnum, is not preserved in any of the available specimens. The rather small foramen vagi is visible on the left exoccipital of MNHN F BR 4020, whereas the foramen for cranial nerve XII may be represented by a tiny pore and the lateral carotid foramen by a much larger opening located below these two foramina; in MNHN F BR 13106 both the lateral carotid foramina are situated at the level of the ventral edge of the missing condyle (as well as at the dorsal edge of the basisphenoid). The ventral projections of the exoccipitals along the lateral sides of the basioccipital do not reach the weakly developed basioccipital tubera.

Basioccipital: The basioccipital makes up the occipital condyle and more ventrally, the basioccipital plate. The basioccipital has the shape of a truncated trapezoid pointing ventrally, with a prominent sagittal crest developed in the ventral sector of the occipital surface. The condyle is entirely developed in this element: it is neither massive nor large relative to the rest of the element. The two preserved condyles (MNHN F BR 4020, MNHN F BR 4119) have a distinct sagittal depression at their dorsal edge. The location of the lateral Eustachian canal corresponds to an evident notch in the lateral profile of the basioccipital. In the skull MNHN F BR 13105, the basioccipital seems to develop a knob instead of the sagittal crest and the two tubercle-like structures, placed laterodorsally to this knob, do not have an equivalent in the other available specimens (the surface of MNHN F BR 13105 is however markedly altered and not clearly visible).

Basisphenoid: The basisphenoid is best preserved in MNHN F BR13105. The expansion of the basisphenoid ventral to the medial Eustachian foramen is clearly visible from a posterior view. This bone expands ventrally and sends a broad sheet on the pterygoid. It connects anteriorly with the pterygoid and more laterally contacts the quadrate and even the medioventral tip of the exoccipital. On the lateral side of the braincase, the basisphenoid is anteroposteriorly wide and its dorsal edge is at the level of the lateral carotid foramen (best seen in MNHN F BR 4020). The lateral carotid foramina open dorsally relative to the median Eustachian foramen.

Prootic: The prootic is visible from the left side of CE 00001 but is not visible in other skulls from MNHN F because of crushing of the area. Although visible on the ventral and posterior margin of the foramen ovale, its exposure remains limited. The pterygoid contacts the ventral surface of this foramen. The quadrate makes up the posterior margin of the foramen ovale and extends further ventrally to meet the pterygoid. The dorsal margin of the foramen ovale is occupied by the quadrate, which projects anteriorly to meet the laterosphenoid.

Laterosphenoid: The laterosphenoid is also visible from the left side. It makes up the anterior-most margin of the foramen ovale. The bone widens in its anterodorsal portion. It is however largely fragmented but despite this its general shape remains visible.

Mandible

Dentary: The dentary is elongate and represents more than two thirds of the mandibular length. It contributes to the anterior portion of the external mandibular fenestra. It also comprises the anterodorsal portion of this fenestra, contacting the surangular near the middle of the fenestra. In lateral view, the tooth row is not linear but is gently festooned. The first concavity occurs between the first and third alveoli and is short. Long and gentle (i.e. longer than deep) concavities expand between the fourth and the tenth alveoli, then behind the 14th alveolus for a similar length. The dentary symphysis is long and attains the level of the fourth alveolus in MNHN F BR 4021 and the fifth alveolus in CE 00001, MNHN F BR 2617, and MNHN F BR 13216. The anterior portion, lateral to the symphysis is, together with the symphysis profile, almost horizontal. The dentary hosts 20 alveoli, the last two being crushed and obscured medially in CE 00001, but clearly preserved in MNHN F BR 2617 and 13216. The first alveolus is large and is separated from the next one by a diastema. The third and fourth alveoli are the same size and confluent. Their margin is elevated relative to the tooth row. Alveoli 5 to 10 are slightly smaller and of similar size. Alveoli 11 and 12 are as large as the first alveolus and the confluent teeth. They are followed by nine alveoli, the diameters of which progressively decrease caudally. The last alveoli tend to become mediolaterally compressed. At least in CE 00001, the medial rims of the posterior-most alveoli receive a contribution of the splenial. Lateral to alveoli 15, 16, and 17 are occlusal pits affecting the surface of the dentary of CE 00001. No trace of occlusal pits could be detected elsewhere on the dentary. The maxillary teeth occlude labially to the mandible, with the posterior-most dentition tending to occlude closer to the mandibular tooth row except for the maxillary interalveolar space between the seventh and eighth alveoli, and possibly the adjacent ones, which occlude in line.

Splenial: The splenial clearly forms part of the symphysis of the lower jaw (Figs 5, 7A, B, E, F) and frames the Meckelian groove (foramen for cranial nerve V branch) with a ventral and a dorsal process both of similar anterior extensions [visible in several specimens including MNHN F BR 15150 (Fig. 7E, F) and CE 00001 (Fig. 5)]. Medially, the splenial almost hides the dentary. Even though the foramen for the mandibular ramus of cranial nerve V is not entirely surrounded by the splenial, this element is here considered as anteriorly perforate. Caudally, the splenial becomes elevated and eventually builds the medial alveolar wall from the level of the 15th alveolus. From the 13th alveolus to its posterior end, the splenial is thickened where it is in contact with the last alveoli.

Coronoid: These elements are not preserved either in connection with other elements or isolated. None of the related characters can be assessed because even the scars on the surrounding elements are not visible with confidence.

Surangular: The lateral profile of the surangular is low and also gives a low profile to the posterior mandibular ramus. The anterodorsal process of the surangular is forked and is almost free of sculptural pits. It does not reach far anteriorly and stops well before the level of the posterior tooth row. The medial process of the fork tapers slightly more anteriorly than the lateral process. The posterolateral area of the surangular is densely covered with large pits. The surangular meets the dentary on the dorsal portion of the external mandibular fenestra. The suture with the angular occurs at the posterior level of the same fenestra. The surangular sends a posterior process that reaches to the tip of the retroarticular process (Fig. 8). This is supported by the sutural surface of isolated articulars that develops nearly entirely on the articular edge, indicating that the surangular nearly reached the tip of the process. It also sends a dorsal lamina that nearly reaches the tip of the lateral wall of the glenoid fossa. A shallow fossa lies ventrally to this lamina. From an occlusal view, the area for insertion of the M. adductor mandibulae superficialis and medius is wide. The lingual foramen for the articular artery and alveolar nerve is not visible in the medial surface of four of the five available surangulars; the fifth (MNHN F BR 1675) has a small perforation.

Angular: The angular makes up all of the posteroventral portion of the mandible. It participates in most of the ventral and posterior margin of the external mandibular fenestra. This fenestra is quite large but not large enough that the medial process of the angular is visible. On the medial side, the angular participates in the ventral and dorsal margins of the foramen intermandibularis caudalis (Fig. 5), the dorsal tip being shorter than the ventral tip. Therefore, the splenial only contacts this foramen anteriorly.

Articular: The articular is remarkable: the construction of the retroarticular process is similar to that of *Leidyosuchus* but unlike that of many extant crocodilians. The process is long and slightly concave and thus projects somewhat posterodorsally. However, it is located in a ventral position relative to the jaw joint. This condition is not as extreme as in some basal short-snouted alligatorines, such as *Arambourgia gaudryi*

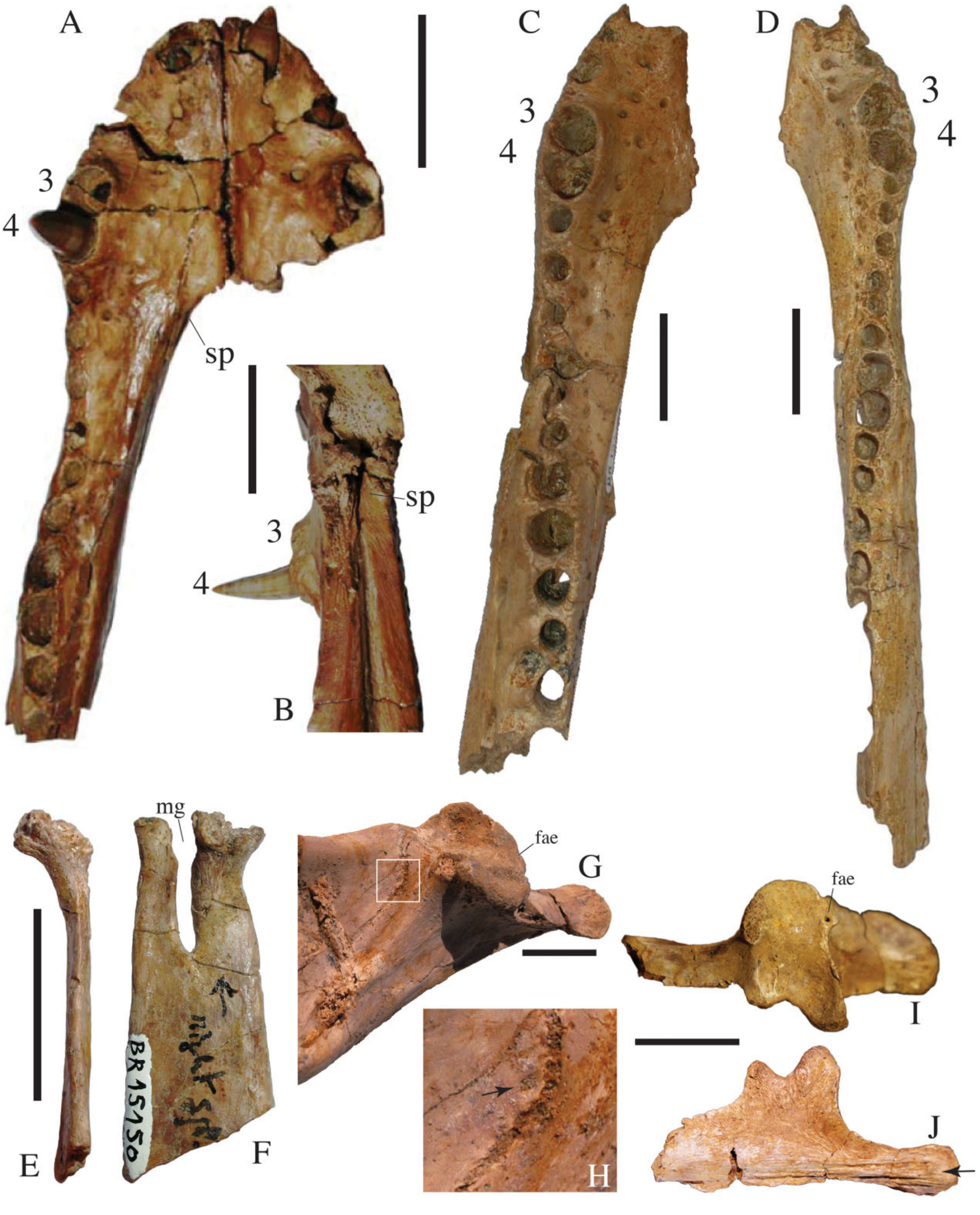

Figure 7. Anatomical details of the mandible of ***Diplocynodon remensis* sp. nov.** from the Late Palaeocene of Mont de Berru, Marne, France. Left and partial anterior right ramus of IRSNB R289 in A, dorsal and B, medial views with an emphasis on the splenial symphysis. Left and right dentaries in dorsal view of C, MNHN F BR 15198, and D, MNHN F BR 13216. E, F, right splenial of MNHN F BR 15150. G, lingual foramen of CE 0001; H, close-up. I, left articular in dorsal and J, lateral views (MNHN F BR 3596); the arrows shows the posterior-most area suturing with the surangular. Abbreviations: 3, 4, tooth or alveolus position in the maxilla or dentary; fae, foramen aëreum; mg, Meckelian groove; sp, splenial; Scale bars = 2 cm.

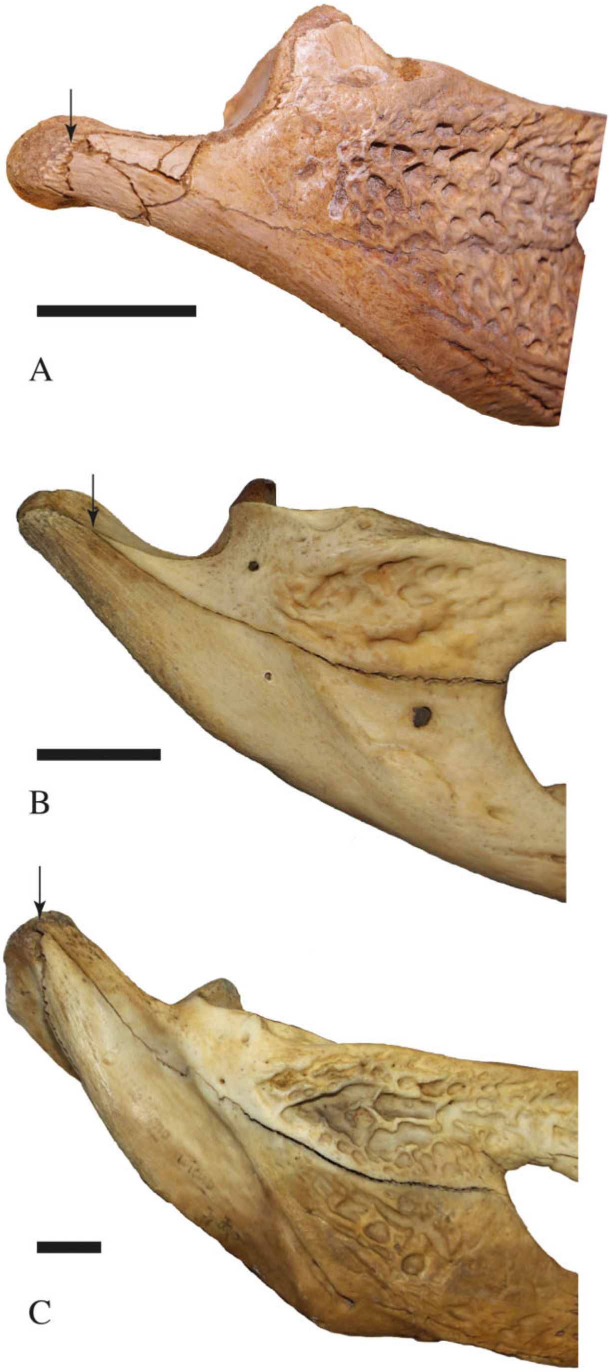

Figure 8. Comparison of the sutural extent of the surangular (indicated by an arrow) on the posterior tip of the retroarticular process, in right lateral view in A, ***Diplocynodon remensis* sp. nov.** (CE 0001); B, *Alligator mississippiensis* (MHNL 50.001396); and C, *Crocodylus niloticus* (MHNL 50.001387). Note that in A, the posteriormost tips of the surangular and angular are damaged but their extension is indicated by the sutural area visible on the articular. Scale bars = 2 cm.

de Stefano, 1905, *Hassiacosuchus haupti* Weitzel, 1935, or *Krabisuchus siamogallicus* Martin & Lauprasert, 2010, in which the process originates from the ventral portion of the articular. The articular lateral fossa is three times wider than the medial one for reception of the lateral and smaller medial quadrate condyles. The angular and surangular meet dorsally of the anterior process of the articular. The articular–surangular suture along the medial wall of the lower jaw is not developed inside a groove because the articular surface is flush against the medial surface of the surangular. The lingual foramen for the articular artery and alveolar nerve does not pierce the articulars and probably opens along the articular–surangular suture, as indicated by the weak depression in MNHN F BR 10146. In MNHN F BR 1675, MNHN F BR 13206, and CE 0001, the surangular is pierced by this lingual foramen close to the articular suture. The descending ramus of the articular does not spread anteriorly on the medial surface of the surangular (in MNHN F BR 1675 it is not significantly directed in an anterior direction dorsally to the foramen). The foramen aëreum (Fig. 7I) is situated along the posterior rim of the glenoid surface (on the crest that separates it from the retroarticular cavity) and markedly set in from the medial edge of the articular.

Dentition

A large number of isolated teeth has been collected from Cernay-les-Reims and they can be assigned to *D. remensis* based on the characteristics described below. In some cases, a single individual preserves most of the teeth and therefore it is possible to evaluate variation in tooth morphology. This is the case for CE 00001, in which teeth are present in most alveoli. The premaxillary and maxillary teeth show a similar morphology. They are of the classic conical shape bearing carinae on the mesiodistal surface and are all curved lingually. Their surface is smooth (although a hint of longitudinal ridges is present). The posterior maxillary teeth have smaller crowns but remain conical. In all teeth assignable to *D. remensis*, the passage from crown to root is marked by a faint constriction (Fig. 9). The crown can display numerous transverse lines representing the continuous growth lines of the tooth. The colour of these lines alternates from light to dark. As far as the MNHN F collection is considered, a limited number of teeth is preserved on the teeth-bearing bones. Nearly no complete teeth are preserved on the two skulls BR 13105 and BR 4020 or in the lower jaws (Figs 1, 2, 7B), but an informative sample of tooth morphologies is offered by the isolated maxillae. The fragmentary maxilla BR 13711 preserves three teeth from the anterior region (second, third, and fifth) showing a rather slender, variably curved, and pointed shape: the largest tooth (the fifth but the size of the fourth alveolus is

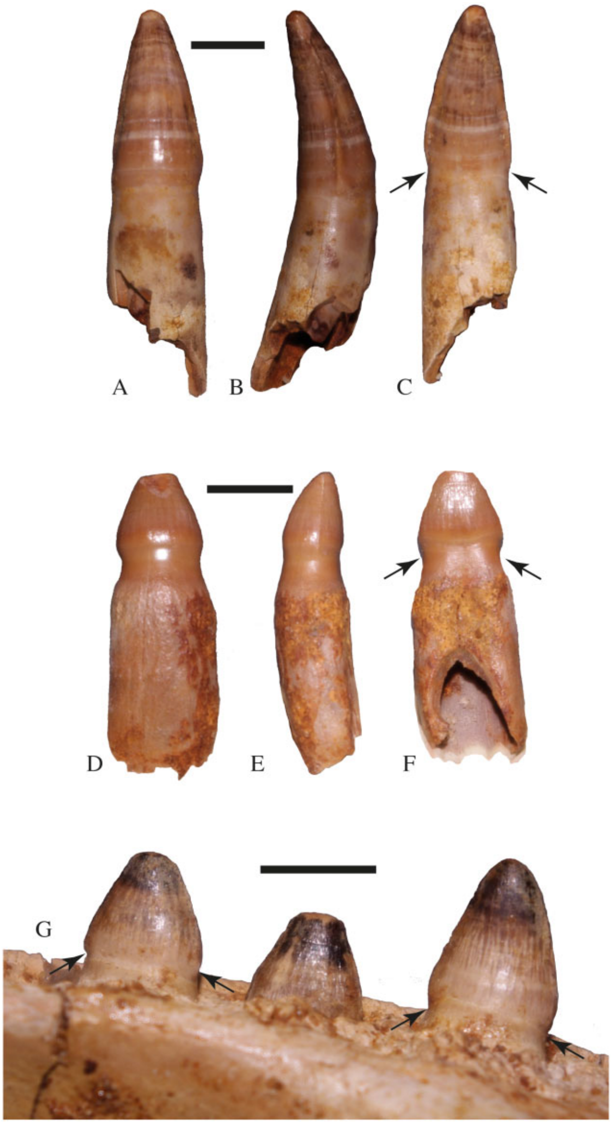

Figure 9. The dentition of ***Diplocynodon remensis* sp. nov.** (un-numbered MNHN specimens). Isolated tooth from the anterior region of the dentition in A, labial, B, mesial, and C, lingual views; isolated tooth from the posterior region in D, labial, E, mesial, and F, distal views. G, detail of the posterior maxillary teeth of MNHN F BR 13207 in lingual view. Arrows indicate the crown/root constriction, from where the mesiodistal carinae of the crown begin to expand. Scale bars = 0.5 cm.

approximately the same as that of the fifth) has a crown 15 mm tall and 7.8 mm wide at the base (mesiodistal diameter). The mesiodistal ridges are smooth and well developed: they delimit a small lingual and large labial surface. The posterior teeth are less elongated, not curved, and rather stout (the 12th tooth of specimen BR 13207 is 5.8 mm tall –it is slightly worn apically – and 6.8 mm wide at the base) but both the keels and the surfaces are nearly smooth (a hint of longitudinal ridges is sometimes present). Both the anterior and posterior teeth show a weak but evident constriction at the base of the crown (Fig. 9).

Pattern of occlusion: With only one exception, occlusal pits are hardly visible on the maxillae from Mont de Berru. In the anterior region, small and shallow pits are present in the median sector (and partly medially to it) of at least interalveolar spaces two and five of BR 13711, whereas specimen BR 13207 has pits more developed and more medially placed, corresponding to interalveolar spaces two, five and six. A well-marked pit is however present between alveoli 7 and 8 in all of the best-preserved maxillae (CRL 13099, BR 3486, BR 2636, BR 13207; in the left maxilla of the skull BR 4020 interalveolar pits are present before and after alveolus 7 – the condition is not assessable for the right element because of the poor state of preservation). In the posterior region, only specimen CRL 13099 has a modest pit slightly medial to the interalveolar space nine. Maxilla BR 13207 has a shallow depression situated in the medial sector of the interalveolar space after the eighth tooth and partly medial to it; medially to the following two or three interalveolar spaces, the shallow depressions (separated by irregular convexities) may possibly represent weakly defined occlusal pits. The same could be said for the pits visible medially to interalveolar spaces 8 and 9 in the left maxilla of the skull BR 4020 (the posterior region is not preserved). More convincing evidence for the occlusal pattern of the Mont de Berru crocodylian is offered by the lower jaws. Evident pits are located lateral (but the most anterior one is also significantly developed in the medial sector of the interalveolar space) to the 13th to 16th alveoli in the best-preserved specimen, BR 13216. Similar conditions are seen in specimens BR 4021 and BR 15230 and, at least for the preserved anterior sector, in BR 13218 and BR 15198. The nicely preserved dentary BR 2617 is distinctly smaller than the others (nearly completely preserved – total length 15 cm) and shows just the hint of a pit laterally to the 14th and 15th alveoli. It is therefore likely that the development of this character is related to body size.

The occlusion pattern shown by the Mont de Berru crocodylian is therefore the one in which all the dentary teeth occlude lingually to the maxillary ones with the exception of the dentary tooth corresponding to the seventh maxillary interalveolar space and possibly the adjacent ones that occlude in line.

Osteoderms

Numerous (about 300) isolated osteoderms have been collected in Mont de Berru. Their ornamentation is, as in the skull elements described above, made up of a uniform and dense net of deep and well-delimited

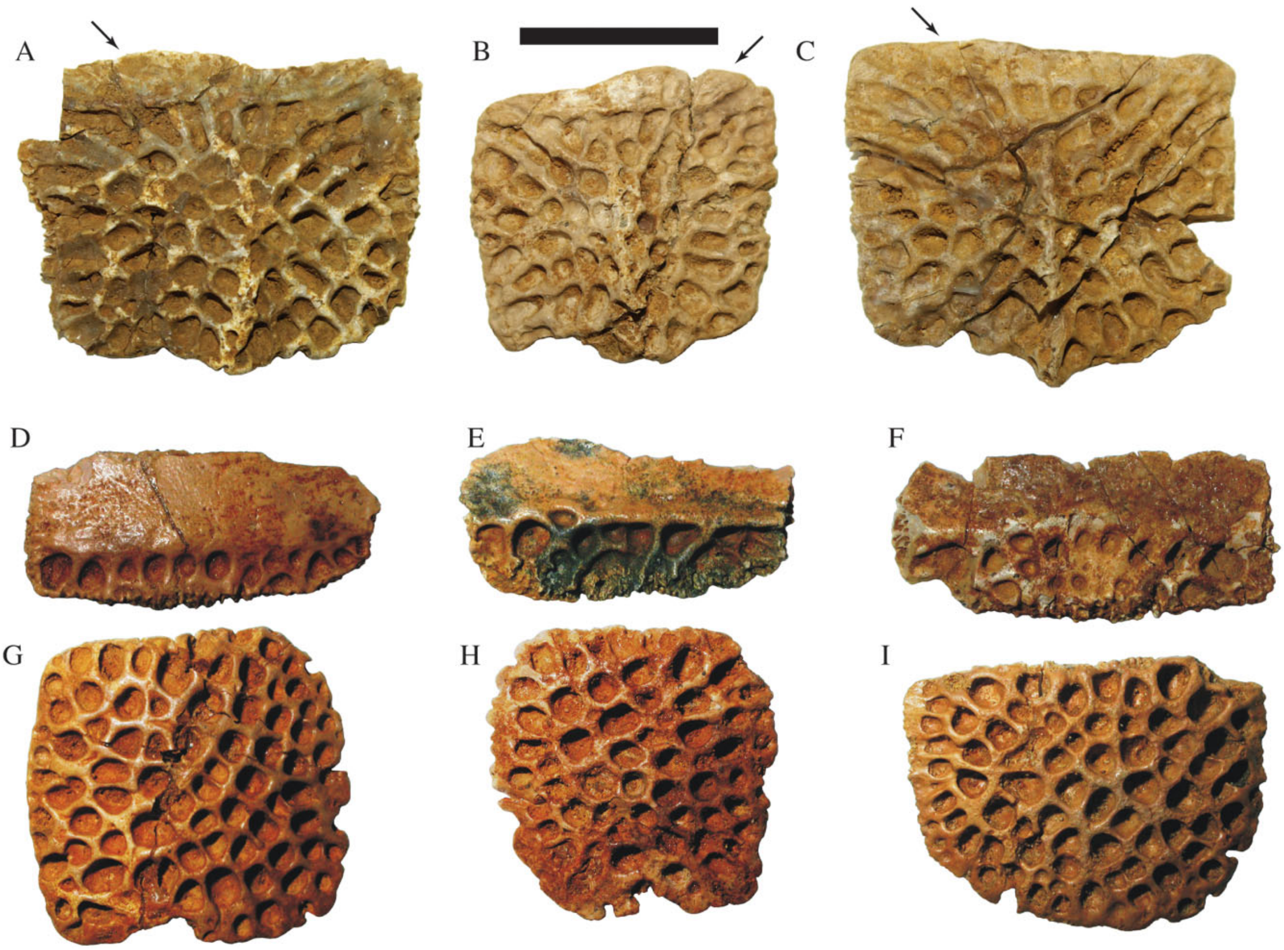

Figure 10. Selected osteoderms attributed to ***Diplocynodon remensis* sp. nov.** Dorsal osteoderms showing the anterolateral process (arrows): A, MNHN F BR 3466; B, MNHN F BR 15106; and C, MNHN F BR 2658. Bipartite ventral osteoderms: anterior half: D, MNHN F BR 154176; E, MNHN F BR 17412; and F, MNHN F BR 3467; posterior half: G (MNHN F BR 15481); H (MNHN F BR 15084); and I (MNHN F BR 15480). Scale bar = 2 cm.

pits surrounded by narrow ridges. The preserved specimens cover all of the different regions of the dermal armour. The cervical elements (such as MNHN F BR 3432) are characterized by a longitudinal ridge (not situated in the centre of the osteoderm) that represents a line of ventral bent. The dorsal elements (Fig. 10A–C) are usually markedly keeled and rectangular in shape; according to their medial or lateral position, they show sutures along both lateral and medial edges or simply on the medial edge. The cranial end of all of the dorsal osteoderms has a clearly visible articular facet. Here, the anterior margin is concave and a wide anterolateral process is visible in most specimens (Fig. 10A–C). The ventral osteoderms are bipartite and suture together (Char. 39-2 in Brochu *et al.*, 2012b). Both types are rather flat and devoid of any keel: the anterior ones (Fig. 10D–F) are broad and anteroposteriorly narrow, with a smooth anterior surface usually developed on more than half of the surface; the sutural surface (at the lateral and caudal edges) is slightly inclined, and therefore partly visible in external view, the external (ornate) surface of the osteoderm being slightly smaller than the internal (smooth) one. The posterior ventral (Fig. 10G-I) elements are characterized by having a ventral surface completely ornate; the anterior edge typically has a well-developed sutural surface.

PHYLOGENETIC ANALYSIS

METHODS

Diplocynodon remensis was scored and included in the data matrix of Brochu *et al*. (2012b) for eusuchians, which contained a total of 97 taxa and 179 characters (Supporting Information Appendix S1). The most complete species of *Diplocynodon* are part of this data matrix: *Diplocynodon darwini*, *Diplocynodon deponiae*, *Diplocynodon hantoniensis*, *Diplocynodon ratelii*, *Diplocynodon muelleri*, *Diplocynodon tormis*, and now *D. remensis*. Another analysis was conducted here and included two more, albeit less complete species of *Diplocynodon*, *Diplocynodon elavericus* and *Diplocynodon ungeri*, which were included in previous analyses (Martin, 2010; Martin & Gross, 2011) and were recoded in the present study to fit into the data matrix of Brochu *et al.* (2012b). Character 103, concerning the ectopterygoid–maxillary suture, was updated for all species of *Diplocynodon* according to previous work on diplocynodontid phylogeny (Martin & Gross, 2011; Delfino & Smith, 2012). Replicates of 1000 random addition sequences were performed under TNT (Goloboff, Farris & Nixon, 2003). *Bernissartia fagesii* was defined as the outgroup taxon as in Brochu *et al.* (2012b). For clarity of reading, the strict consensus tree presented here (Fig. 11) has been simplified for some clades (i.e. Gavialoidea, Globidonta, and Crocodyloidea). Character codings are presented in the Appendix.

RESULTS

The analysis retained 30 trees [best tree length = 656; consistency index (CI) = 0.3410; retention index (RI) = 0.8087]. The retrieved topology follows the one by Brochu *et al.* (2012b). Previous analyses recovered a polytomy amongst *D. deponiae*, *D. darwini*, *D. hantoniensis*, and a clade containing *D. ratelii*, *D. muelleri*, and *D. tormis* (Brochu *et al.*, 2012b). The present analysis recovered *D. darwini* as the basalmost diplocynodontid followed by *D. deponiae*, followed by *D. remensis*, *D. hantoniensis*, and *D. ratelii*, and then by the couple *D. muelleri* plus *D. tormis*. A Bremer decay analysis required two steps longer than the optimal tree to collapse Crocodyloidea and Alligatoroidea (other indexes are reported on the simplified Fig. 11). Diplocynodontidae are especially well supported, with a Bremer decay value of 1. Basal members of the crown group (i.e. Gavialoidea and *Borealosuchus*) are fairly well supported, with a Bremer decay value of 2.

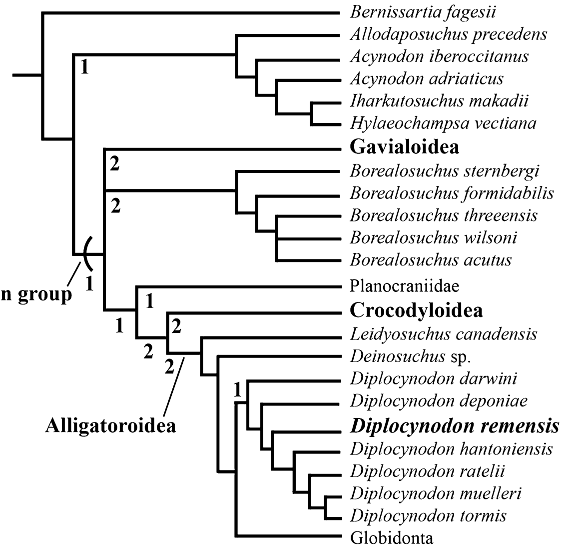

Figure 11. Strict consensus tree resulting from the inclusion of ***Diplocynodon remensis* sp. nov**. in the framework of the Eusuchia. Bold numbers refer to Bremer decay indices.

The second analysis, which also included the less complete species of *Diplocynodon* (*D. elavericus* and *D. ungeri*), shows the same arrangement as the above analysis with the exception of a polytomy involving all Diplocynodontidae and *Deinosuchus* sp. Here, a strict consensus of 30 trees yielded a shortest tree length of 689 steps (CI = 0.3295; RI = 0.799).

DISCUSSION

EARLIEST DIPLOCYNODONTIDS

The Palaeocene fossil record of eusuchians is far from being complete, with *D. remensis* representing the most complete material from Europe. The inclusion of a set of nearly complete skulls and mandibles from a single late Palaeocene locality of Europe in the most up-to-date phylogenetic framework of the Eusuchia (Brochu *et al.*, 2012b) led to the hypothesis that this material represents the oldest diplocynodontid member. *Diplocynodon* was erected by Pomel (1847) on the basis of material from the Miocene of Saint-Gérand le Puy, Allier, France. Several occurrences of the genus were subsequently reported from Cenozoic and also Cretaceous localities in North America (Mook, 1960; Parris *et al.*, 1997). All of these North American finds were eventually assigned either to *Leidyosuchus* or to *Borealosuchus* (Brochu, 1997). Brochu (1999) considered the presence of double caniniforms in the maxillary and dentary dentition as a plesiomorphic character, an interpretation supported by its presence in the outgroup to Eusuchia, the Goniopholididae (e.g. Schwarz, 2002; Brochu, 2004b). On the basis of this plesiomorphic character, several authors referred the fragmentary material from the MP6 of Mont de Berru to *Diplocynodon* sp. or aff. *Diplocynodon* sp. (Ginsburg & Bulot, 1997; Pereda-Suberbiola *et al.*, 1999; Hua, 2004). The previously recognized oldest remains of *Diplocynodon* were reported from the earliest Eocene (MP7) of Silveirinha (Telles-Antunes & Russell, 1981), Dormaal (Godinot *et al.*, 1978; Buffetaut, 1985), and Le Quesnoy (Hua, 2004). As is the case for Cernay, the latter attribution was based on isolated dentary bones bearing two confluent alveoli, enlarged and subequal in size, and although this character is present in *Diplocynodon*, more material is needed to test whether or not they really belong to this genus. The above description of numerous remains from Mont de Berru together with the phylogenetic results seem to support the occurrence of *Diplocynodon* at the locality of Mont de Berru, but as highlighted below, this result is not clear-cut. The nesting of *D. remensis* within the clade Diplocynodontidae does not have stratigraphical congruence, because being the oldest representative of that group, *D. remensis* would be expected to fall as the basal-most member. Instead, it sits in an intermediate position. This is perplexing given that *D. remensis* has a peculiar morphology that clearly differentiates it from other diplocynodontids: it is the only member of Diplocynodontidae that possesses a splenial participating in the mandibular symphysis. Nevertheless, it is not the first time that stratigraphical incongruence with phylogenetic results has been observed for *Diplocynodon* (Martin, 2010; Martin & Gross, 2011; Delfino & Smith, 2012). Future work should address this.

COMPARISON OF *D. REMENSIS* WITH BASAL-MOST ALLIGATOROIDS

Diplocynodon remensis shares with all members of the genus *Diplocynodon* the following character combination diagnostic of this group (Martin, 2010; Martin & Gross, 2011): a pair of enlarged maxillary (four and five) and confluent dentary (three and four) alveoli; the extent of the lacrimal, which is longer than the prefrontal; the ectopterygoid adjacent to the posterior-most alveoli; and the dorsal margin of the infratemporal fenestra formed by the quadratojugal, preventing the quadrate from reaching the fenestra. Between 17 and 18 maxillary alveoli are also present in all of these taxa. Nevertheless, *D. remensis* differs in the participation of the splenial in the dentary symphysis, which has never before been documented for any member of the genus *Diplocynodon* (see Delfino & Smith, 2012, for a discussion of the splenial in *D. deponiae*). With the exception of the maxillary alveolus count and the extent of the lacrimal, the characters mentioned above in the diagnosis of *Diplocynodon* are also present in the genus *Borealosuchus*.

Diplocynodon remensis and *Leidyosuchus canadensis* are similar in many (non-exclusive) respects, the most striking being the position of the foramen aëreum (a derived character diagnosing Alligatoroidea) and the exclusion of the anterior process of the nasal from the external nares (as seen in other species of *Diplocynodon*). Other similarities (compare with the detailed illustrations in Wu *et al*., 2001) include the general outline of the skull, both being mesorostral forms, a maxillary count of 18 alveoli (17–18 in *Diplocynodon*), the possession of double caniniform dentary alveoli occluding in a marked notch at the level of the premaxillary–maxillary suture, the long mandibular symphysis, extending to the level of the fifth dentary alveolus, and other general patterns such as ornamentation, size of orbits, supratemporal fenestra, relative position of lacrimal and prefrontal, involvement of the splenial in the dentary symphysis, and position of the retroarticular process. However, substantial differences distinguish these two taxa. For example, in *Leidyosuchus*, the external mandibular fenestra is much smaller, the pterygoid does not project anteriorly between the suborbital fenestrae, and the anterior palatine process is long and rectangular in shape.

Identification in alligatoroids of a lateral pit or a notch at the level of the premaxillo–maxillary suture has received particular attention. This character allows extant crocodyloids to be distinguished from alligatoroids, the latter having a pit for the reception of the occluding fang-like dentary tooth, which sometimes can erode the lateral wall of the rostrum at the premaxillary–maxillary suture (e.g. Norell, Clark & Hutchison, 1994; Brochu, 1999). An interesting case is Owen (1849–1884) who erected two separate species, *Crocodilus hastingsiae* and *Alligator hantoniensis* based on the presence/absence of this feature, which were later revealed to be from the same species: *D. hantoniensis*. Therefore, until recently, all of the species of the genus *Diplocynodon* were thought to display this ontogenetic variation of a pit becoming a notch, as testified by rich ontogenetic series of at least *D. ratelii* and *D. darwini* (see amongst others, Brochu, 1999; Delfino & Sánchez-Villagra, 2010). However, in *D. remensis*, the morphology of the lateral edge of the snout at the premaxillary–maxillary suture can be confidently viewed as a notch for several reasons. The notch is deep, larger than the diameter of a single caniniform tooth. The morphology in *D. remensis* does not resemble the condition sometimes observed in *Caiman*, in which a pit becomes a notch as the result of occluding erosion. In the small specimen MNHN F BR15012, the notch is already present and well delineated, indicating that early in ontogeny this feature already had the morphology of a notch in *D. remensis*.

COMPARISON OF *D. REMENSIS* WITH *BOREALOSUCHUS*

Previous preliminary studies on the taxon described in the present work gave controversial results and assigned this material to *Borealosuchus* (Martin, 2008), or recognized a close relationship with some members of *Borealosuchus* (Martin *et al*., 2012). Nevertheless, the most current phylogenetic hypotheses (including this one) have recovered *Borealosuchus* as distantly related to *Diplocynodon*. In the present study, none of the authors had the opportunity to examine specimens referred to *Borealosuchus* first-hand and for this reason, comparisons were made solely upon published accounts and might need updating with future revisions. Comparison of *D. remensis* with species of *Diplocynodon* and *Borealosuchus* reveals some similarities in these two distantly related lineages (currently understood as homoplasies). Highlighting these characters may prove useful when revising or describing species of *Borealosuchus* in the future. *Diplocynodon remensis* displays features absent from the other *Diplocynodon* species but which have so far been viewed as unique features of the genus *Borealosuchus*, or of some species of *Borealosuchus*. The anterior extent of the nasals is broadly separated from the naris by a substantial portion of the premaxillae in *D. remensis* and in all species of *Borealosuchus* (Brochu, 1997, 1999; Wu *et al*., 2001). By contrast, the nasals almost contact the naris in some species of *Diplocynodon* (e.g. *D. darwini* in fig. 32 of Brochu, 1999). The surangular of *D. remensis* extends to the posterior end of the retroarticular process, a condition identical to the genus *Borealosuchus* according to the diagnoses of Brochu (1997) and Wu *et al*. (2001). The wall of the premaxillary–maxillary notch of *D. remensis* bears a recess (Fig. 6H–J) as in *B. griffithi* (Wu *et al*., 2001: fig. 11A). This feature has never been documented in other species of either *Borealosuchus* or *Diplocynodon*.

Some other characters indicate that *D. remensis* shares features only with certain species of *Borealosuchus*. For example, the splenial of *D. remensis* participates in the posterior region of the mandibular symphysis as in *B. sternbergii* (Gilmore, 1910), *B. formidabilis* (Erickson, 1976), and *B. griffithi* (Wu *et al*., 2001) but unlike in *Borealosuchus* sp. from Black Peaks (Brochu, 2000), *B. wilsoni*, and *B. threeensis* (Brochu *et al*., 2012b). The extent of the lacrimal varies in the genus *Borealosuchus*. Wu *et al*. (2001) reported that the relative position of the anterior tips of the prefrontal and lacrimal is more similar in *B. griffithi* and *B. sternbergii* than it is in other species of *Borealosuchus*. The condition in *D. remensis* (although the skulls have suffered from compression that may have impacted the suture positions), with the prefrontal shorter than the lacrimal but still tapering relatively far anteriorly, recalls the condition of *B. griffithi* (see fig. 2 in Wu *et al*., 2001) and *B. sternbergii* (according to Wu *et al*., 2001). It should also be noted that the shapes of the retroarticular process and of the external mandibular fenestra in *D. remensis* closely resemble the morphology in *B. sternbergii* and *B. formidabilis*, but not the morphology of *B. wilsoni* or *B. threeensis* (see comparative fig. 5 in Brochu *et al*., 2012b). *Diplocynodon remensis*, *B. sternbergii*, and *B. formidabilis* all have relatively large external mandibular fenestrae and a short retroarticular process whereas *B. wilsoni* and *B. threeensis* have an almost closed external mandibular fenestra and a posterodorsally expanded retroarticular process. The retroarticular process is unknown in *B. griffithi*, but the external mandibular fenestra is comparable in size and shape to that of *D. remensis*, *B. sternbergii*, and *B. formidabilis*.

Brochu (2000) and Brochu *et al*. (2012b) pointed out the presence of an anterolateral process in dorsal osteoderms of *Borealosuchus* sp. from Black Peaks, *B. threeensis*, and in general in the genus *Borealosuchus*. Brochu *et al*. (2012b) interpreted the combination of these osteoderms with the presence of double caniniform dentary dentition as characteristic of *Borealosuchus* and stated that this character is unique to the genus *Borealosuchus* (Brochu et *al*., 2012b: 110). Our description reveals that although the pattern of cupular ornamentation is more pronounced in *D. remensis* than in *Borealosuchus*, the osteoderms of this taxon also display an anterolateral process, as in *Diplocynodon* (J. E. Martin & M. Delfino, pers. observ.) but also recalling that described in *Borealosuchus* (Brochu *et al*., 2012b), and to some extent the morphology for basal crocodyloids or even tomistomines (C. A. Brochu, pers. comm., 2014).

BIOGEOGRAPHY OF EARLIEST DIPLOCYNODONTIDS

The presence of the crocodilian *D. remensis* in the late Palaeocene of Mont de Berru indicates that the genus *Diplocynodon* already occurred in Europe before the PETM. This European occurrence contrasts with that of modern placental mammals and most North American immigrants that reached Europe later, around the time of the PETM and which belong to the same lineages as Northern European species (Smith, Rose & Gingerich, 2006). As a comparison, several groups of archaic placental mammals, such as phenacodontids, nyctitheriids, apatemyids, and pantodonts, known from the Palaeocene in North America, first occurred in Europe during the earliest Eocene and presumably dispersed from North America. This mammalian dispersal took place around the PETM about 56 Mya, and is correlated with the first occurrences of the earliest modern placental mammals, such as primates, perissodactyls, and artiodactyls that appeared suddenly on all three continents of the Northern Hemisphere (Smith *et al*., 2006). Some North American groups of lizards and birds share strong similarities with European ones during the early Eocene (Mayr, 2009; Smith, 2009; Rage, 2012). Palaeocene continental localities in Europe are indeed limited, but their faunistic content is rich for some groups and well studied. For example, turtle taxa are more numerous in Mont de Berru than other vertebrate groups, as well as at Eocene times, in France (Broin, 1977; Groessens-Van Dyck, 1982; Pérez-García, 2012). They show a faunal turnover after the Palaeocene at the PETM. Most belong to laurasiatic cryptodiran families present as well in Asia and North America, but their genera are different in Europe and North America, endemic in Europe, and showing an

Asiatic origin (Lapparent de Broin, 2001; Hervet, 2004a, b, 2006). Moreover, with respect to other crocodilians, the locality of Mont de Berru also includes an *Asiatosuchus*-like taxon (Vasse, 1992, 1993; Delfino & Smith, 2009) unknown from North America but bearing possible Asiatic affinities.

By contrast, the co-occurrence in Mont de Berru of the plesiadapid *Plesiadapis*, the arctocyonid *Arctocyon*, and the multituberculate *Neoplagiaulax*, three genera well known from the Palaeocene of North America, does not exclude a pre-PETM dispersal from North America in the late Palaeocene, anterior to Mont de Berru and Menat, for associated faunas including a form closely allied to *Diplocynodon*. The capacity for mammals to disperse by land is greater than that of freshwater vertebrates because of their locomotor capacity. However, this dispersal capacity cannot be excluded for freshwater crocodilians, able to perform high-walk (Zug, 1974) to search for new drainages.

A second hypothesis is that *Diplocynodon* was already endemic to Europe before the late Palaeocene, a possibility already suggested by previous phylogenetic results (e.g. Martin & Buffetaut, 2008) and that could be further tested if the lost *Menatalligator bergouniouxi* Piton, 1940, from the middle/late Palaeocene of Auvergne, France, can be located. Favouring this last hypothesis, another group with North American affinities recently recovered in the Palaeocene of Menat (?Selandian–?Thanetian) and previously known in the Late Palaeocene of Mont de Berru under the name of *Compsemys* (Late Cretaceous–Middle Palaeocene of North America) is the paracryptodiran turtle *Berruchelus russelli* Pérez-García, 2012.

In conclusion, even if according to the results of this research diplocynodontids were already present in Europe in the late Palaeocene, therefore before the PETM, the precise timing of their dispersals, or that of their ancestor if a local evolution is assumed, remain unsettled. A better knowledge of the Palaeocene alligatoroids from North America and, above all, a direct comparison with their European contemporaries would help in clarifying these issues.

ACKNOWLEDGEMENTS

B. Battail, R. Allain (MNHN), and A. Folie (IRSNB) provided access to fossil crocodilian collections and assisted us while studying the collections under their care. G. Lenglet (IRSNB) kindly provided extant comparative materials. A. Pérez-García (Madrid) discussed with us the geographical affinities of the chelonian taxa from Berru. M. Pavia (Torino) provided relevant literature. J. E. M. also thanks E. Buffetaut for earlier discussions, D. Berthet (Musée des Confluences de Lyon) for providing access to specimens and G. de Ploëg for advice during mechanical preparation of CE 0001. Financial support for this research was received from Le Conseil Général de l'Allier (PhD funding to J. E. M.), the Federal Science Policy Office of Belgium (projects MO/36/020 and BR/121/A3/PALEURAFRICA to T. S.), Spanish Ministerio de Economia y Competitividad (CGL2011-28681 to M. D.), 'Fondi ex-60%' (University of Torino to M. D.), and the SYNTHESYS Project (http://www.synthesys.info/), the latter of which is funded by European Community Research Infrastructure Action under the FP6 and FP7 'Structuring the European Research Area' Programme (BE-TAF 2788 to J. E. M. and FR-TAF 967, BE-TAF 4907, GB-TAF-3097 to M. D.). The reviewers M. Rabi and C. A. Brochu provided constructive comments and criticisms that significantly improved the quality of this work. Finally, we warmly thank S. Cedolin for organizing the acquisition of the CT scan of CE 0001.

REFERENCES

Agassiz L. 1849. Remarks on the Crocodilia of the Greensand of New Jersey and on *Atlantochelys*. *Proceedings of the Academy of Natural Sciences of Philadelphia* **4:** 1–169.

Aubry M-P, Thiry M, Dupuis C, Berggren WA. 2005. The Sparnacian deposits of the Paris Basin: a lithostratigraphic classification. *Stratigraphy* **2-1:** 65–100.

Biochro'M. 1997. Actes du Congrès BiochroM'97. In: Aguilar J-P, Legendre S, Michaux J, eds. *Mémoires et Travaux de l'Ecole Pratique des Hautes Etudes, Institut Montpellier*. Vol. 21. Ecole Pratique des Hautes Etudes: Montpellier, 769–805.

Brochu CA. 1997. A review of '*Leidyosuchus*' (Crocodyliformes, Eusuchia) from the Cretaceous through Eocene of North America. *Journal of Vertebrate Paleontology* **17:** 679–697.

Brochu CA. 1999. Phylogenetics, taxonomy, and historical biogeography of Alligatoroidea. *Society of Vertebrate Paleontology Memoirs* **6:** 9–100.

Brochu CA. 2000. *Borealosuchus* (Crocodylia) from the Paleocene of Big Bend National Park, Texas. *Journal of Paleontology* **74:** 181–187.

Brochu CA. 2004a. Alligatorinae phylogeny and the status of *Allognatosuchus* Mook, 1921. *Journal of Vertebrate Paleontology* **24:** 857–873.

Brochu CA. 2004b. A new Late Cretaceous gavialoid crocodilian from eastern North America and the phylogenetic relationships of thoracosaurs. *Journal of Vertebrate Paleontology* **24:** 610–633.

Brochu CA. 2006a. A new miniature horned crocodile from Quaternary of Aldabra Atoll, Western Indian Ocean. *Copeia* **2006:** 149–158.

Brochu CA. 2006b. Osteology and phylogenetic significance of *Eosuchus minor* (Marsh 1870), new combination, a longirostrine crocodylian from the Late Paleocene of North America. *Journal of Paleontology* **80:** 162–186.

Brochu CA. 2013. Phylogenetic relationships of Palaeogene ziphodont eusuchians and the status of *Pristichampsus* Gervais, 1853. *Earth and Environmental Science, Transactions of the Royal Society of Edinburgh* **103:** 521–550.

Brochu CA, Denton RK, Grandstaff BS, Schein JP. 2012a. Southern northern crocodiles: *Borealosuchus* from the Campanian of Alabama and the early biogeographic history of crocodylians in North America. *Journal of Vertebrate Paleontology* Supplement **2:** 68A.

Brochu CA, Parris DC, Smith Grandstaff B, Denton RK, Gallagher WB. 2012b. A new species of *Borealosuchus* (Crocodyliformes, Eusuchia) from the Late Cretaceous–early Paleogene of New Jersey. *Journal of Vertebrate Paleontology* **32:** 105–116.

Buffetaut E. 1985. Les crocodiliens de l'éocène inférieur de Dormaal (Brabant, Belgique). *Bulletins de la Société Belge de Géologie* **94:** 51–59.

De Bast E, Smith T. 2013. Reassessment of the small arctocyonid *Prolatidens waudruae* from the early Paleocene of Belgium, and its phylogenetic relationships with primitive ungulates. *Journal of Vertebrate Paleontology* **33:** 964–976.

De Broin F. 1977. Contribution à l'étude des Chéloniens. Chéloniens continentaux du Crétacé et du Tertiaire de France. *Mémoires du Muséum National d'Histoire Naturelle* **C38:** 1–366.

Delfino M, Codrea V, Folie A, Dica P, Godefroit P, Smith T. 2008b. A complete skull of *Allodaposuchus precedens* Nopcsa, 1928 (Eusuchia) and a reassessment of the morphology of the taxon based on the Romanian remains. *Journal Vertebrate Paleontology* **28:** 111–122.

Delfino M, Martin JE, Buffetaut E. 2008a. A new species of *Acynodon* (Crocodylia) from the Upper Cretaceous (Santonian-Campanian) of Villaggio del Pescatore, Italy. *Palaeontology* **51:** 1091–1106.

Delfino M, Piras P, Smith T. 2005. Anatomy and phylogeny of the gavialoid *Eosuchus lerichei* from the Paleocene Europe. *Acta Palaeontologica Polonica* **50:** 565–580.

Delfino M, Sánchez-Villagra MR. 2010. A survey of the rock record of reptilian ontogeny. *Seminars in Cell and Developmental Biology* **21:** 432–440.

Delfino M, Smith T. 2009. A reassessment of the morphology and taxonomic status of '*Crocodylus*' *depressifrons* Blainville, 1855 (Crocodylia, Crocodyloidea) based on the Early Eocene remains from Belgium. *Zoological Journal of the Linnean Society* **156:** 140–167.

Delfino M, Smith T. 2012. Reappraisal of the morphology and phylogenetic relationships of the alligatoroid *Diplocynodon deponiae* (Frey, Laemmert and Riess, 1987), based on a three-dimensional specimen. *Journal of Vertebrate Paleontology* **32:** 1358–1369.

Dollo L. 1907. Nouvelle note sur les reptiles de l'Eocène inférieur de la Belgique et des régions voisines (*Eosuchus lerichei* et *Eosphargis gigas*). *Bulletin de la Société belge de Géologie, Paleontologie et Hydrologie* **21:** 81–85.

Domingo L, López-Martínez N, Soler-Gijón R, Grimes ST. 2007. A multi-proxy geochemical investigation of the early Palaeocene (Danian) continental palaeoclimate at the Fontllonga-3 site (South Central Pyrenees, Spain). *Palaeogeography, Palaeoclimatology, Palaeoecology* **256:** 71–85.

Erickson BR. 1976. Osteology of the early eusuchian crocodile *Leidyosuchus formidabilis*, sp. nov. *Monograph of the Science Museum of Minnesota (Paleontology)* **2:** 1–61.

Erickson BR. 1982. *Wannagosuchus*, a new alligator from the Paleocene of North America. *Journal of Paleontology* **56:** 492–506.

Erickson BR. 1998. Crocodilians of the Black Mingo Group (Paleocene) of the South Carolina Coastal Plain. *Transactions of the American Philosophical Society, New Series* **88:** 196–214.

Gilmore CW. 1910. *Leidyosuchus sternbergii*, a new species of crocodile from the Cretaceous Beds of Wyoming. *Proceedings of the United States National Museum* **38:** 485–502.

Ginsburg L, Bulot C. 1997. Les *Diplocynodon* (Reptilia, Crocodylia) de l'Orléanien (Miocène inférieur à moyen) de France. *Geodiversitas* **19:** 107–128.

Gmelin J. 1789. *Linnei Systema Naturae*. Leipzig: G. E. Beer.

Godfriaux I, Thaler L. 1972. Note sur la découverte de dents de mammifères dans le Montien continental du Hainaut (Belgique). *Bulletins de l'Académie Royale de Belgique Classe des Sciences* **58:** 536–541.

Godinot M, de Lapparent de Broin F. 2003. Arguments for a mammalian and reptilian dispersal from Asia to Europe during the Paleocene-Eocene boundary interval. *Deinsea* **10:** 255–275.

Godinot M, de Lapparent de Broin F, Buffetaut E, Rage J-C, Russell D. 1978. Dormaal: une des plus anciennes faunes éocènes d'Europe. *Comptes Rendus de l'Académie des Sciences, Paris, Série D* **287:** 1273–1276.

Goloboff PA, Farris JS, Nixon K. 2003. TNT: tree analysis using new technologies Program and documentation available from the authors and at: http://www.zmuc.dk/public/phylogeny

Groessens-Van Dyck MC. 1982. Note sur les chéloniens et les crocodiles du Gisement Paleocène de Vinalmont (Province de Liège, Belgique). *Bulletin de la Société Belge de Géologie* **91:** 163–185.

Groessens-Van Dyck MC. 1986. Les crocodiliens du gisement « Montien » continental de hainin (Hainaut, Belgique) et leur environnement faunique. *Annales de la Société royale zoologique de Belgique* **116:** 55–60.

Hervet S. 2004a. Systématique du groupe « *Palaeochelys* sensu lato – *Mauremys* » (Chelonii, Testudinoidea) du tertiaire d'Europe occidentale: principaux résultats. *Annales de Paléontologie* **90:** 13–78.

Hervet S. 2004b. A new genus of « Ptychogasteridae » (Chelonii, Testudinoidea) from the Geiseltal (Lutetian of Germany). *Comptes Rendus Palevol* **3:** 125–132.

Hervet S. 2006. The oldest European ptychogasterid turtle (Testudinoidea) from the lowermost Eocene amber locality of Le Quesnoy (France, Ypresian, MP7). *Journal of Vertebrate Paleontology* **26:** 839–848.

Hua S. 2004. Les crocodiliens du Sparnacien (Eocene inférieur) du Quesnoy (Oise, France). *Oryctos* **5:** 57–62.

Huxley TH. 1875. On *Stagonolepis robertsoni*, and on the evolution of the Crocodilia. *Quarterly Journal of the Geological Society* **31:** 423–438.

Iordansky NN. 1973. The skull of the Crocodylia. In: Gans C, Parson TS, eds. *Biology of the Reptilia,* vol. 1*, morphology A*. London and New York: Academic Press, 201–262.

Lambe LM. 1907. On a new crocodilian genus and species from the Judith River Formation of Alberta. *Transactions of the Royal Society of Canada* **4:** 219–244.

Lapparent de Broin F. 2001. The European turtle fauna from the Triassic to the Present. *Dumerilia* **4:** 155–216.

Leidy J. 1852. Description of *Delphinus conradi* and *Thoracosaurus gradis*. *Proceedings of the Academy of Natural Sciences of Philadelphia* **6:** 35.

Martin JE. 2007. New material of the Late Cretaceous globidontan *Acynodon iberoccitanus* (Crocodylia) from southern France. *Journal of Vertebrate Paleontology* **27:** 362–372.

Martin JE. 2008. New material of the alleged oldest *Diplocynodon* from the Late Paleocene of northeastern France: revision and implications for crocodylian dispersal. In: Dyke G, Naish D, Parkes M, eds. *Fifty-sixth Symposium of Vertebrate Palaeontology and Comparative Anatomy abstracts*. Dublin: The National Museum of Ireland, 58.

Martin JE. 2010. A new species of *Diplocynodon* (Crocodylia, Alligatoroidea) from the Late Eocene of the Massif Central, France, and the evolution of the genus in the climatic context of the Late Palaeogene. *Geological Magazine* **147:** 596–610.

Martin JE, Benton MJ. 2008. Crown clades in vertebrate nomenclature: correcting the definition of Crocodylia. *Systematic Biology* **57:** 173–181.

Martin JE, Buffetaut E. 2008. *Crocodylus affuvelensis* Matheron, 1869 from the Late Cretaceous of southern France: a reassessment. *Zoological Journal of the Linnean Society London* **152:** 567–580.

Martin JE, Delfino M. 2010. Recent advances on the comprehension of the biogeography of Cretaceous European eusuchians. *Palaeogeography, Palaeoclimatology, Palaeoecology* **293:** 406–418.

Martin JE, Delfino M, de Broin F, Escuillié F, Smith T. 2012. Greenhouse world, high latitude dispersal and the origin of the alligatoroid *Diplocynodon*. In: *Abstract book 4th International Geologica Belgica Meeting – Moving Plates and Melting Icecaps – Processes and Forcing Factors in Geology*. Brussels, Belgium, September 2012, 114.

Martin JE, Gross M. 2011. Taxonomic clarification of *Diplocynodon* Pomel, 1847 (Crocodilia) from the Miocene of Styria, Austria. *Neues Jahrbuch für Geologie und Paläontologie – Abhandlungen* **261:** 177–193.

Martin JE, Lauprasert K. 2010. A new primitive alligatorine from the Eocene of Thailand: relevance of Asiatic members to the radiation of the group. *Zoological Journal of the Linnean Society* **158:** 608–628.

Mayr G. 2009. *Paleogene fossil birds*. Berlin: Springer-Verlag.

Mook CC. 1959. A new species of fossil crocodile of the genus *Leidyosuchus* from the Green River Beds. *American Museum Novitates* **1933:** 1–6.

Mook CC. 1960. *Diplocynodon* remains from the bridger beds of Wyoming. *American Museum Novitates* **2007:** 1–4.

Norell MA, Clark JM, Hutchison JH. 1994. The Late Cretaceous alligatoroid *Brachychampsa montana* (Crocodylia): new material and putative relationships. *American Museum Novitates* **3116:** 1–26.

Owen R. 1849–1884. *A history of British fossil reptiles.* Volume 2. London: Casell and Company Limited.

Parris DC, Barbara S, Denton RK Jr, Dobie JL. 1997. *Diplocynodon* (Alligatorinae) in the Cretaceous of Eastern North America. *Journal of Vertebrate Paleontology* Supplement **17:** 69A.

Peláez-Campomanes P, López-Martínez IN, Álvarez-Sierra MA, Daams R. 2000. The earliest mammal of the European Paleocene: the multituberculate *Hainina*. *Journal of Paleontology* **74:** 701–711.

Pereda-Suberbiola X, Murelaga X, Astibia H, Badiola A. 1999. Restos fósiles del cocodrilo *Diplocynodon* (Alligatoroidea) en el Mioceno inferior de las Bardenas Reales de Navarra. *Revista Española de Paleontología* **16:** 223–242.

Pérez-García A. 2012. *Berruchelus russelli*, gen. et sp. nov., a paracryptodiran turtle from the Cenozoic of Europe. *Journal of Vertebrate Paleontology* **32:** 545–556.

Piton LE. 1940. Paléontologie du gisement éocène de Menat (Puy-de-Dôme) (flore et faune). *Mémoires de la Société d'Histoire Naturelle* **1:** 1–303.

Pomel A. 1847. Note sur les animaux fossiles découverts dans le département de l'Allier. *Bulletin de la Société Géologique de France* **4:** 378–385.

Rage J-C. 2012. Amphibians and squamates in the Eocene of Europe: what do they tell us? *Palaeobiodiversity and Palaeoenvironments* **92:** 445–457.

Rauhe M, Rossmann T. 1995. News about fossil crocodiles from the middle Eocene of Messel and Geiseltal, Germany. *Hallesches Jahrbuch für Geowissenschaften* **17:** 81–92.

Russell DE. 1964. Les mammifères paléocènes d'Europe. *Mémoires du Muséum National d'Histoire Naturelle* **C13:** 1–324.

Schwarz D. 2002. A new species of *Goniopholis* from the upper Jurassic of Portugal. *Palaeontology* **45:** 185–208.

Simpson GG. 1930. *Allognathosuchus mooki*, a new crocodile from the Puerco Formation. *American Museum Novitates* **445:** 1–16.

Smith KT. 2009. A new assemblage of squamates from the earliest Eocene (zone Wa0) of the Bighorn Basin, Wyoming: biogeography during the warmest interval of the Cenozoic. *Journal of Systematic Palaeontology* **7:** 299–358.

Smith T, Quesnel F, De Ploëg G, De Franceschi D, Métais G, De Bast E, Solé F, Folie A, Boura A, Claude J, Dupuis C, Gagnaison C, Iakovleva A, Martin J, Maubert F, Prieur J, Roche E, Storme J-Y, Thomas R, Tong H, Yans J, Buffetaut E. 2014. First Clarkforkian equivalent Land Mammal Age in the latest Paleocene basal Sparnacian facies of Europe: fauna, flora, paleoenvironment and (bio)stratigraphy. *PLoS ONE* **9:** e93249.

Smith T, Rose KD, Gingerich PD. 2006. Rapid Asia-Europe-North America geographic dispersal of earliest Eocene primate *Teilhardina* during the Paleocene-Eocene Thermal Maximum. *Proceedings of the National Academy of Sciences, USA* **103:** 11223–11227.

Stefano G. 1905. Apunti sui batraci e rettili del Quercy appartenenti alla collezioni Rossignol. *Bolletino della Societa Geologia Italiana* **24:** 17–67.

Sternberg CM. 1932. A new fossil crocodile from Saskatchewan. *The Canadian Field-Naturalist* **44:** 128–133.

Telles-Antunes M, Russell DE. 1981. Le gisement de *Silveirinha* (Bas Mondego, Portugal): la plus ancienne faune de Veretébrés éocènes connue en Europe. *Comptes Rendus de l'Académie des Sciences, Paris, Série 3* **293:** 773–776.

Thaler L. 1977. Etat des recherches sur la faune de mammifères du Montien de Hainin (Belgique). *Geobios Mémoire Spécial* **1:** 57–58.

Vasse D. 1992. Un crâne *d'Asiatosuchus germanicus* du Lutétien d'Issel (Aude). Bilan sur le genre Asiatosuchus en Europe. *Geobios* **25:** 293–304.

Vasse D. 1993. Systématique de crocodiles du Crétacé supérieur et du Paléogène d'Europe. Aspects paléobiogéographiques et paléoécologiques. DPhil Thesis, Paris: University of Paris 6.

Weitzel K. 1935. *Hassiacosuchus haupti* n. g. n. sp. ein durophages Krokodil aus dem Mitteleozan von Messel. *Notizblatt des Vereins für Erdkunde und der hessischen geologischen Landesanstalt zu Darmstadt* **16:** 40–49.

Wu X-C, Brinkman DB, Fox RC. 2001. A new crocodylian (Archosauria) from the basal Paleocene of the Red Deer River Valley, southern Alberta. *Canadian Journal of Earth Science* **38:** 1689–1704.

Young CC. 1964. New fossil crocodiles from China. *Vertebrata Palasiatica* **5:** 199–208.

Young CC. 1982. *A Cenozoic crocodile from Huaining, Anhui. Selected works of Yang Zhungjian*. Beijing: Science Press, 47–48.

Zarski M, Jakubowski G, Gawor-Biedowa E. 1998. The first Polish find of Lower Paleocene crocodile *Thoracosaurus* Leidy, 1852: geological and palaeontological description. *Geology Quarterly* **42:** 141–160.

Zug GR. 1974. Crocodilian galloping: an unique gait for reptiles. *Copeia* **1974:** 550–552.

APPENDIX

Character codings used in the present phylogenetic work. Character list (179 discrete morphological characters) and definitions as in Brochu *et al*. (2012b).

DIPLOCYNODON REMENSIS SP. NOV.

?????????????????????????????????????10??20???0100 2000?????0 1110?00011 1001????00?20?000000 0131000000 100???1??? 0000001101 0001010000 1?1100???0 1000000010 10110100???1?1??0100 110010001

DIPLOCYNODON ELAVERICUS

?????????????????????????????????????10???0???0?10 2??1????????1????0?1???1????1? 1??????10? 1131??000??00??????? 1001100101 10?101?0?0 1?1?0??????10?1110?0 0021?110???0???11?0??0?11???0

DIPLOCYNODON UNGERI

?????????????????????????????????????1????????0110 210100?010 0010101??? 110?????0? 120??00000 0?3000000???0??????? 0001110011???1010000 111?00?100 010??11200 0??1?112???0????0?0????01???1

SUPPORTING INFORMATION

Additional Supporting Information may be found in the online version of this article at the publisher's web-site:

Movie S1. Digitally rendered skull of *Diplocynodon remensis* sp. nov. obtained from a computed tomography scan of CE 0001.

Movie S2. Digitally rendered mandible of *Diplocynodon remensis* sp. nov. obtained from a computed tomography scan of CE 0001.

Appendix S1. Data matrix used in the phylogenetic analysis.